

SOLUTION OF THREE-DIMENSIONAL VISCOUS COMPRESSIBLE FLOW THROUGH A RECTANGULAR DUCT BY IMPLICIT FINITE DIFFERENCE METHOD

by

AMIT SAHAY

T₁
AE/1993/m

AE Sa 195
1993

M
SAH
Soh



DEPARTMENT OF AEROSPACE ENGINEERING
INDIAN INSTITUTE OF TECHNOLOGY KANPUR

FEBRUARY 1993

SOLUTION OF THREE-DIMENSIONAL VISCOUS COMPRESSIBLE
FLOW THROUGH A RECTANGULAR DUCT BY IMPLICIT FINITE
DIFFERENCE METHOD

A Thesis Submitted
in Partial fulfilment of the requirements
for the degree of
Master of Technology

by

AMIT SAHAY

To the

DEPARTMENT OF AEROSPACE ENGINEERING
INDIAN INSTITUTE OF TECHNOLOGY, KANPUR

FEBRUARY, 1993

07 APR 1993

CENTRAL LIBRARY
IIT KANPUR

No. A.15420

H 115420

Th

629.134354

Sc 19 A

AE-1993-M-SAH-SOL

18/2/93

P. Mohi

CERTIFICATE

It is certified that the work contained in the thesis entitled
" SOLUTION OF THREE-DIMENSIONAL, VISCOUS, COMPRESSIBLE FLOW
THROUGH A RECTANGULAR DUCT BY IMPLICIT FINITE DIFFERENCE METHOD"
by Amit Sahay, has been carried out under my supervision and that
this work has not been submitted elsewhere for a degree.

O P Sharma
(Dr. O. P. Sharma)
Department of Aerospace Engineering
I.I.T. Kanpur

ABSTRACT

While solving internal flow equations near the inlet/starting stage, it is not always desirable to incorporate simplifying assumptions. In the past two decades some numerical schemes have been reported, in the literature, to solve multidimensional compressible Navier Stokes equations. A generalized implicit finite difference method with increased computational efficiency has been developed by W.R. Briley and H. McDonald [1].

In this method the governing equations are replaced by its implicit time difference approximations. Terms involving non-linearities at the implicit time level are linearized by Taylor expansion about their solution, at the known time step. This results in a system of coupled equations which are linear for the dependent variables. Alternating Direction Implicit (ADI) technique is applied to the linearized equations. Here ADI technique developed by Douglas-Gunn has been applied. Application of ADI technique leads to equations which are one-dimensional. These equations are replaced by their finite difference approximations using the standard central difference formula. The finite difference equations when applied to successive grid points give rise to block-tridiagonal and tridiagonal systems of equations which are solved by standard methods.

The method, illustrated above, is applied to solve the flow field through a rectangular duct being fed through a stagnant reservoir of fluid at one end and a specified pressure at the

downstream end. The primary aim is to predict the detailed compressible, three-dimensional flow field to establish the validity of the computer code, developed for this purpose. The computer code may be used for solving flow field in intakes and in solid rocket thrust chambers. Computations have been done by varying the input parameters to determine their effect on the flow field as well as the limitations of the method, if any.

ACKNOWLEDGEMENTS

wish to express my deep gratitude to Dr. O. P. Sharma for his able guidance towards the successful completion of this work. I am thankful to the teachers of I. I. T. Kanpur who imparted me with a strong background for research work.

I am thankful to Amitabh Mukherjee, Prashant Deb, Peeyush Shankar Arg, K. C. Navneet Kumar, Manoj T. Nair, Atul Rathore, P. Subodhaen, Manmohan Pandey, K. M. Singh, Uday Shankar Dixit and Seena Pant for the special interest they showed in this work.

I owe my enjoyable stay in I. I. T. to Peeyush Vaish, Vinayak Ugru, Arag Kumar and Bhabhiji, A.K.S. Nagarkoti, S. C. Pradhan, N. Sudhakar, I. Sridhar, S. S. Rao, Surajit Roy, Venu Madhav, Anubhav Tripathi, Parthasarathi Mandal, Sanjay Srivastava, D. N. Singh, Govind Swarup Pathak, Y. P. Singh, Rakesh Kr. Verma, Rajan Gurjar, Manish Agarwal, Nisha Bawa, Vandana Gupta, Anupama Astogi, Sonal Khare, Manjari Srivastava, Kumar, Rajiv Mahajan, Jagendra Goel, Hemant Priyadarshi, Amitabh Gupta, Rajesh Khanna, Bhuvnesh Singh, Shaikhant Khanna, Lovraj Gupta, Ashok Kumar, Partha Pratim Dey, Alok Sharan, S. K. Verma, Shaligram Tiwari, Sunil Garg, Amarnath Reddy, Samuel Jones, Suhash Chand Mishra, Raj Srivastava, Alok Tiwari, Shankar Shiva, Dewashish Mishra, Rajan Chand, Shamsi, Mukul Kulshrestha, Shekhar Shukla, Sanjay Pathak, Hemant Kumar, Chetan Kumar, Sailesh Tiwari, Prashant Shukla, Manish Garg, Pramod Kumar Choudhary, Kanu Tripathi, M.N. Singh, Bhauhan, Anand Prasad Gupta, Rajesh Kr. Pathak, Abhijit Sur, Banaria, S.P. Chandrashekhar, Deepak Gupta, Prem Shankar, A. K. Lohra, Joseph, Ashish Balaya, J. Venkatesh, Venkat Reddy, Swami, Krishna Raman, Ashwin Vaishnav, Sanjay Shah, Jayesh Sharma, Md. Iaved, Sarvesh Srivastava and Rajiv Ranjan Prasad.

I really enjoyed the company of my friends from M.I.T., Nizaffarpur, Himanshu Shekher, Prakash Kumar, Ashok Kumar Choudhary, Vikas Kumar, Kailas Kumar, Sanjay Singh, Sujit Kumar and Shailendra Mohan Singh.

C O N T E N T S

	Page No.
Title	(i)
Certificate	(ii)
Abstract	(iii)
Acknowledgements	(v)
Contents	(vi)
Notations	(viii)
List of figures	(xi)
Chapter 1 INTRODUCTION	1
1.1 General background	1
1.2 Present investigation	4
Chapter 2 PROBLEM FORMULATION	6
2.1 Physical description of flow field	6
2.2 Governing equations	6
2.3 Boundary conditions	.
2.4 Non dimensionalisation of equations	9
Chapter 3 NUMERICAL METHOD	12
3.1 General outline	12
3.2 Finite difference equations for the governing equations	12
3.3 Finite difference equations for the boundary equations	21
3.4 Solution procedure for the finite difference equations	25
3.5 Tridiagonal form	31
3.6 Initial conditions	32

Chapter 4	RESULT AND DISCUSSIONS	34
Chapter 5	FUTURE WORK	47
APPENDIX I		48
APPENDIX II		49
APPENDIX III		52
REFERENCES		53

NOTATIONS

Letters

γ	ratio of the two specific heat of air = 1.4
H	Total enthalpy
H	Total enthalpy(non-dimensionalised)
M	Mach number
p	pressure
p	pressure(non-dimensionalised)
pr	prandtl number
Re	Reynold number
ρ	density
ρ	density(non-dimensionalised)
t	time
t	time(non-dimensionalised)
T	temperature
T	temperature(non-dimensionalised)
u	component of velocity along x
u	component of velocity along x (non-dimensionalised)
v	component of velocity along y
v	component of velocity along y (non-dimensionalised)
w	component of velocity along z
w	component of velocity along z (non-dimensionalised)
x, y, z	axes of Cartesian co-ordinate convention
(x, y, z)	position of a point according to Cartesian co-ordinate convention
x_1, y_1, z_1	height, width, and, length of the duct (non dimensionalised)
$\Delta x, \Delta y, \Delta z$	mesh size along x, y, z respectively

Δt time step

Superscript

n refers to the value of flow variables at known time step

$n+1$ refers to the value of flow variables at unknown time step

$*$ refers to the intermediate solution of flow variables after the first ADI step

$**$ refers to the intermediate solution of flow variables after the second ADI step

T indicates transpose of matrices

Subscript

i refers to the position of grid point along x axis

j refers to the position of grid point along y axis

k refers to the position of grid point along z axis

Others

L_r reference length

U_r reference velocity

T_r reference temperature

ρ_r reference density

\vec{V} velocity vector

\vec{V}' velocity vector (non-dimensionalised)

$\psi_{\rho}^{n+1} - \rho^n$

$\psi_u^{n+1} - u^n$

$\psi_v^{n+1} - v^n$

$\psi_w^{n+1} - w^n$

$\psi_T^{n+1} - T^n$

$\psi^* \{ \psi_{\rho}^* \quad \psi_u^* \quad \psi_T^* \}^T$

P_{stag} stagnation pressure
 T_{stag} stagnation temperature
 P_s static pressure
ADI Alternating Direction Implicit
FIG figure

LIST OF FIGURES

	Page No.
FIG 2.1 Duct geometry and co-ordinate system	7
FIG 4.1 Variation of computed axial velocity along x at $y = 0.5, z = 0$; $P_{stag} = 4.2, P_e = 2.0, T_{stag} = 1.03, Re = 60, M = 0.44$.	36
FIG 4.2 Variation of computed axial velocity along x at $y = 0.5, z = 0.5$; $P_{stag} = 4.2, P_e = 2.0, T_{stag} = 1.03, Re = 60, M = 0.44$.	36
FIG 4.3 Variation of computed centreline velocity with axial distance; $P_{stag} = 4.2, P_e = 2.0, T_{stag} = 1.03, Re = 60, M = 0.44$.	37
FIG 4.4 Variation of computed centreline pressure with axial distance; $P_{stag} = 4.2, P_e = 2.0, T_{stag} = 1.03, Re = 60, M = 0.44$.	37
FIG 4.5 Variation of computed centreline velocity with axial distance; $P_{stag} = 4.2, P_e = 3.15, T_{stag} = 1.03, Re = 60, M = 0.44$.	38
FIG 4.6 Variation of computed centreline pressure with axial distance; $P_{stag} = 4.2, P_e = 3.15, T_{stag} = 1.03, Re = 60, M = 0.44$.	38
FIG 4.7 Variation of computed centreline velocity with axial distance; $P_{stag} = 4.5, P_e = 3.15, T_{stag} = 1.03, Re = 60, M = 0.44$.	39
FIG 4.8 Variation of computed centreline pressure with axial distance; $P_{stag} = 4.5, P_e = 3.15, T_{stag} = 1.03, Re = 60, M = 0.44$.	39
FIG 4.9 Variation of computed centreline velocity with axial distance; $P_{stag} = 6.0, P_e = 3.15, T_{stag} = 1.03, Re = 60, M = 0.44$.	40
FIG 4.10 Variation of computed centreline pressure with axial distance; $P_{stag} = 6.0, P_e = 3.15, T_{stag} = 1.03, Re = 60, M = 0.44$.	40

- FIG 4.11 Variation of computed axial velocity along x at $y = 0.5, z = 0$; $P_{stag} = 5.0, P_e = 3.15, T_{stag} = 1.03, Re = 60, M = 0.44.$ 41
- FIG 4.12 Variation of computed axial velocity along x at $y = 0.5, z = 0.5$; $P_{stag} = 5.0, P_e = 3.15, T_{stag} = 1.03, Re = 60, M = 0.44.$ 41
- FIG 4.13 Variation of computed centreline velocity with axial distance; $P_{stag} = 5.0, P_e = 3.15, T_{stag} = 1.03, Re = 60, M = 0.44.$ 42
- FIG 4.14 Variation of computed centreline pressure with axial distance; $P_{stag} = 5.0, P_e = 3.15, T_{stag} = 1.03, Re = 60, M = 0.44.$ 42
- FIG 4.15 Variation of computed axial velocity along x at $y = 0.5, z = 0$; $P_{stag} = 5.0, P_e = 3.15, T_{stag} = 1.03, Re = 200, M = 0.44.$ 43
- FIG 4.16 Variation of computed axial velocity along x at $y = 0.5, z = 0.5$; $P_{stag} = 5.0, P_e = 3.15, T_{stag} = 1.03, Re = 200, M = 0.44.$ 43
- FIG 4.17 Variation of computed centreline velocity with axial distance; $P_{stag} = 5.0, P_e = 3.15, T_{stag} = 1.03, Re = 200, M = 0.44.$ 44
- FIG 4.18 Variation of computed centreline pressure with axial distance; $P_{stag} = 5.0, P_e = 3.15, T_{stag} = 1.03, Re = 200, M = 0.44.$ 44
- FIG 4.19 Variation of computed centreline velocity with axial distance; $P_{stag} = 4.2, P_e = 3.15, T_{stag} = 1.03, Re = 100, M = 0.44.$ 45
- FIG 4.20 Variation of computed centreline pressure with axial distance; $P_{stag} = 4.2, P_e = 3.15, T_{stag} = 1.03, Re = 100, M = 0.44.$ 45
- FIG 4.21 Variation of computed centreline velocity with axial distance; $P_{stag} = 4.2, P_e = 3.15, T_{stag} = 1.03, Re = 100, M = 0.3$. 46
- FIG 4.22 Variation of computed centreline pressure with axial distance; $P_{stag} = 4.2, P_e = 3.15, T_{stag} = 1.03, Re = 100, M = 0.3$. 46

1. INTRODUCTION

1.1 General background

A set of mathematical equations governing the flow of a compressible, viscous fluid was developed early in the 19th century and subsequently became known as the Navier-Stokes equations. These equations, in the most general form, include the equations of conservation of mass, momentum and energy relating the pertinent dependent variables viz. density, velocity, pressure and temperature which describe the flow of a compressible, viscous and heat conducting fluid. Since that time the basic form of the equations for describing the behavior of a continuous fluid has remained unchanged and form a set of non-linear coupled partial differential equations. The work of subsequent research has been directed at finding approximate or analytic solutions for simple or special flow situations as well as to consider approximate or modified forms of these equations to predict turbulence, heat and mass transfer, shock waves etc. [8]

There are basically three approaches or methods which can be used to predict the behavior of fluid motion. These methods may be grouped as (1) Experimental (2) Theoretical and (3) Numerical. The experimental approach has the capacity of producing the most realistic answers for many flow problems however the costs of measuring equipments etc. are becoming greater everyday as well as there is also the need to refine the measurement techniques for reliable measurements in complex flow cases. Moreover in performing experiments it is not always possible to simulate the true operating conditions of the prototype. In the theoretical approach, simplifying assumptions are usually made in order to make

the problem tractable. The big advantage of the theoretical approach is that general information can be obtained, in many cases, from a simple expression. This approach is quite useful in preliminary design work since reasonable answers can be obtained in a minimum amount of time. However in many problems of practical interest analytical solutions are not possible. In the numerical approach, a limited number of assumptions are made and a high-speed digital computer is used to solve the resulting governing fluid dynamic equations. A parametric study can be easily carried out to study the variations in a given flow situations. [2]

There are basically two numerical approaches, viz. the finite difference method and the finite element method. [9] In the former method, the governing differential equations are approximated in terms of the dependent variables at a finite number of points in the flow field. There are many methods by which this can be achieved. In general, the partial derivatives of dependent variables at a point are replaced by expressions given in terms of their values at the neighboring locations and the distance between them. This procedure gives rise to algebraic equations which are solved simultaneously to obtain the values of dependent variable(s) at different locations.

The finite element formulation is based on the integral statements of the conservation principles. The region under study is divided into a number of finite elements. The variation within the elements is generally taken as linear and the integral statements of the governing conservation equations postulate yields the integral equations that apply for each element. Minimization of the integrals is carried out in order to satisfy the conservation

principles, thereby obtaining the distribution of the variables in the region. However in fluid flow problems finite difference method has been extensively developed and used during the past few decades.

Problems of fluid mechanics may be divided into two categories. Steady state and unsteady state. The former relates to the circumstance when the variables at all points in the region of solution are independent of time. Unsteady state problems relate to the situation when variables in the region of interest vary with time, in addition to location. Time-dependent solutions are of particular importance to manufacturing processes in which the thermal cycle undergone by the material is of interest. Also the start up and shut down of systems such as power plants, furnaces, ovens, rocket motors etc. invariably involve a consideration of transient conduction. Such systems frequently also have fluctuations in the boundary conditions. Steady-state problems are of interest in the long range steady operation of systems, such as power systems, blast furnaces, ovens, reactors and storage units. [9]

Finite difference schemes are further classified as Explicit scheme and Implicit scheme. An Explicit scheme is one in which only one unknown appears in the finite difference equation in a manner which permits its evaluation in terms of other known quantities. An Implicit scheme is one in which more than one unknown appears in the difference equation. This indicates that the formulation would require the simultaneous solution of several algebraic equations involving the unknowns. In both the Explicit and Implicit schemes, depending upon the step-size, the solution may not always converge

Implicit schemes are more stable in the sense that they permit larger values of time step. Hence less computer time is required to obtain a solution. However Implicit formulation is more complicated to cast into a computer code. It requires more calculations at each time level and hence requires larger computer time at each time step than that for explicit schemes. With larger values of time step, the truncation error will be more, and the use of implicit method to follow the exact transients may not be accurate. However for problems in which steady solution is required, the relative time-wise inaccuracy is not important.

Several computer models for predicting three - dimensional, compressible flows have been reported in the literature during the last decade or so. Researchers at Los Alamos, USA, Imperial College, London, and other research workers have developed standard packages of algorithms such as TEACH code , MINT code , etc., some of which are made available on commercial basis.

1.2 Present investigation

In general, most of the flow field analyses are restricted to the steady state situations as well as for simpler geometries especially away from the inlet section. However analysis of the internal flow field near inlet region is important for accurate prediction of the overall behavior of the fluid in several propulsion systems. During the burning of a solid propellant grain in a rocket thrust chamber, the combustion gases move downward at an increasingly higher speed before passing out of the nozzle. At the upstream end of the nozzle, the flow is developing essentially from stagnant conditions and the flow is fully choked at the

throat. The flow in the developing zone has low Reynolds number and also cannot be treated as a fully developed flow. For correct predictions, it is necessary to deal with the flow field in this region which is of low speed and usually three-dimensional depending upon the grain geometry. For this purpose, a computer code for cold flow at low Reynolds number is developed to obtain steady-state solution of unsteady, three-dimensional, compressible Navier-Stokes equation(s) based on a generalized implicit finite-difference scheme due to W.R.Briley and H.McDonald [1].

2. PROBLEM FORMULATION

2.1 Physical description of flow field

The flow under consideration is laminar, subsonic, compressible in the entrance region of a straight duct having rectangular cross section. The duct is fed from a stagnant reservoir. The flow geometry has been shown in fig 2.1

The flow consists of boundary layers on the walls and an inviscid core flow. At some downstream distance the boundary layers grow to fill the duct and the flow becomes fully viscous.

The flow accelerates along the downstream and at some downstream distance the mean Mach no. becomes unity and the flow becomes choked. Depending on the inlet Mach and Reynolds numbers, the flow may become choked either before or after, it becomes fully viscous. Here the duct length is chosen such that the flow at the exit is neither choked nor fully viscous.

The flow is symmetric about the horizontal and vertical planes passing through the duct centreline. Therefore solutions have been computed only for one quadrant of the duct. Symmetry conditions have been imposed on the planes of symmetry.

2.2 Governing equations :-

The conservation equations for a compressible, viscous, heat-conducting, perfect gas, without body forces and external heat addition may be written in the following form. [3]
 (Here i, j and l are being used as tensor indices)

Continuity equation

$$\frac{\partial \rho}{\partial t} + \frac{\partial (\rho u_j)}{\partial x_j} = 0 \quad (2.2.1)$$

Momentum equation

$$\frac{\partial}{\partial t} (\rho u_i) + \frac{\partial}{\partial x_j} (\rho u_i u_j) = - \frac{\partial p}{\partial x_i} + \frac{\partial}{\partial x_j} \tau_{ij} \quad (2.2.2)$$

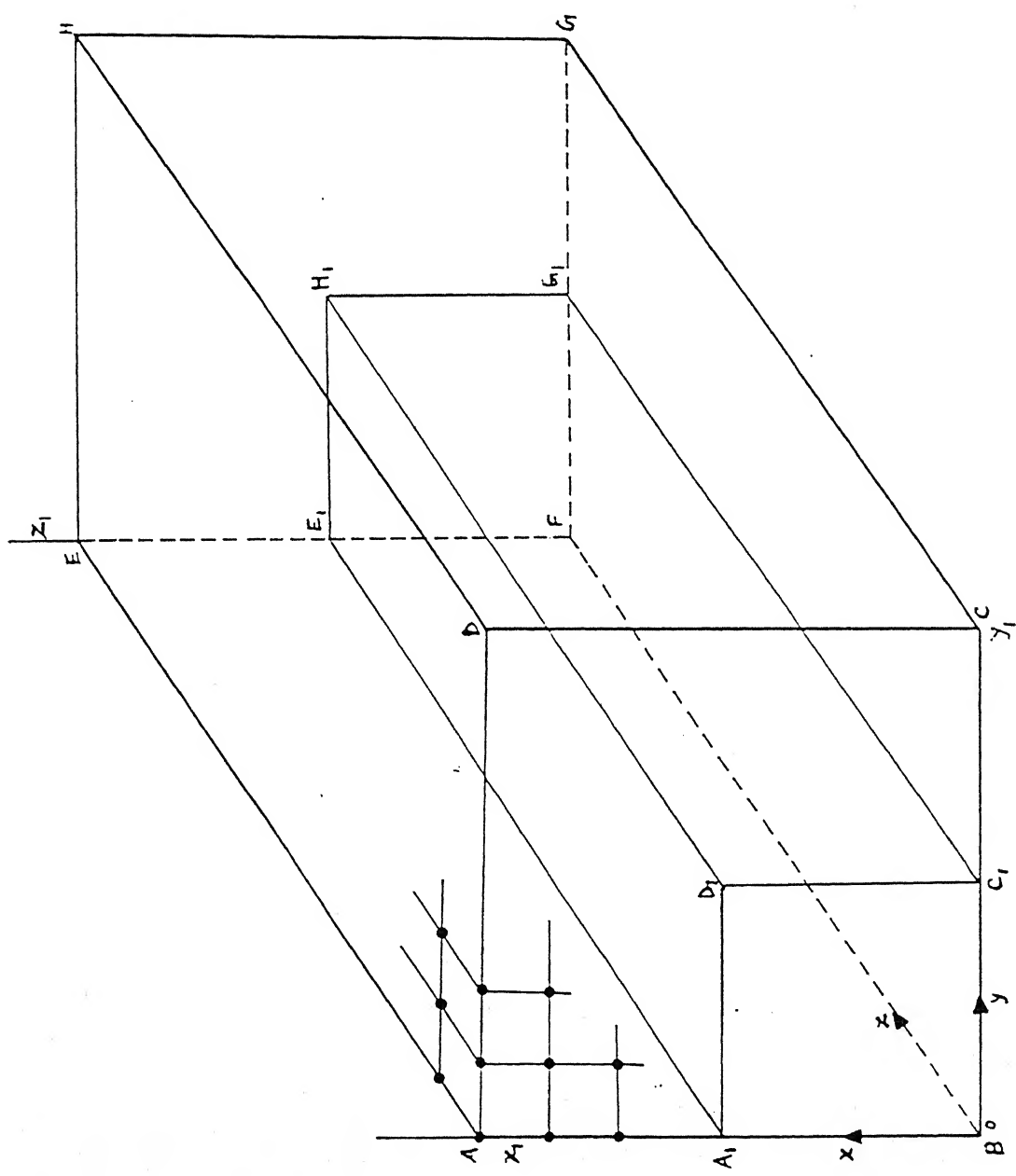


Fig.2.1 Duct geometry and coordinate system

Energy equation

$$\frac{\partial}{\partial t} (\rho H) + \frac{\partial}{\partial x_j} (\rho u_j H) = \frac{\partial p}{\partial t} + \frac{\partial}{\partial x_j} (u_i \tau_{ij} - q_i) \quad (2.2.3)$$

where

$$\tau_{ij} = -\frac{2}{3} \mu \delta_{ij} \frac{\partial u_i}{\partial x_j} + \mu \left(\frac{\partial u_i}{\partial x_j} + \frac{\partial u_j}{\partial x_i} \right)$$

$$q_j = -k \frac{\partial T}{\partial x_j}$$

$$H = h + \frac{1}{2} u_i u_i$$

The pressure can be eliminated as a dependent variable by means of the equation of state for a perfect gas

$$p = \rho R T \quad (2.2.4)$$

2.3 Boundary conditions

Plane BC'G'F

$$u = 0 = v = w \quad \text{(no slip condition)} \quad (2.3.1)$$

$$\frac{\partial T}{\partial x} = 0 \quad \text{(adiabatic condition)} \quad (2.3.2)$$

Density can be determined from the continuity equation, which reduces to $\frac{\partial \rho}{\partial t} + \frac{\partial \rho u}{\partial x} = 0$

Plane A'D'H'E'

$$\frac{\partial \rho}{\partial x} = 0 = \frac{\partial u}{\partial x} = \frac{\partial v}{\partial x} = \frac{\partial w}{\partial x} = \frac{\partial T}{\partial x} \quad (2.3.4)$$

(symmetry conditions)

Plane BA'E'F

$$u = 0 = v = w \quad (2.3.5)$$

$$\frac{\partial T}{\partial y} = 0 \quad (2.3.6)$$

Density can be determined from eqn. (2.2.1) which reduces to

$$\frac{\partial \rho}{\partial t} + \frac{\partial \rho v}{\partial y} = 0 \quad (2.3.7)$$

Plane C'D'H'G

$$\frac{\partial \rho}{\partial y} = 0 = \frac{\partial u}{\partial y} = \frac{\partial v}{\partial y} = \frac{\partial w}{\partial y} = \frac{\partial T}{\partial y} \quad (2.3.8)$$

Plane A'BC'D'

Since the duct is fed from a large stagnant reservoir it is reasonable to assume the flow upstream of the inlet plane as inviscid and adiabatic. Thus constant stagnation temperature and pressure are assumed at the inlet plane.

$$T_{\text{stag}} = T + \frac{1}{2} \frac{w^2}{c_p} \quad (2.3.9)$$

$$\frac{\rho_{\text{stag}}}{\rho} = \left(\frac{T_{\text{stag}}}{T} \right)^{\gamma/(\gamma-1)} \quad (2.3.10)$$

The velocity field at the inlet plane depends on conditions surrounding the inlet. $\frac{\partial w}{\partial z} = 0$ (2.3.11)

has been used as a boundary condition which is compatible with the velocity behavior observed experimentally both in boundary layers and inviscid core region.

The other boundary conditions are

$$\frac{\partial u}{\partial z} = 0 = \frac{\partial v}{\partial z} \quad (2.3.12)$$

Plane E'FG'H'

The duct has an unobstructed exit into a large constant pressure reservoir. So it is reasonable to assume that static pressure at outlet remains constant

$$P_s = \rho R T \quad (2.3.13)$$

and the other boundary conditions may be reasonably taken as

$$\frac{\partial^2 u}{\partial z^2} = 0 = \frac{\partial^2 v}{\partial z^2} = \frac{\partial^2 w}{\partial z^2} = \frac{\partial^2 T}{\partial z^2} \quad (2.3.14)$$

2.4 Non dimensionalisation of equations

The dimensional variables are normalized, with the reference quantities, in the following manner

$$x = x/L_r, y = y/L_r, z = z/L_r, u = u/U_r, v = v/U_r, w = w/U_r$$

$$\rho = \rho_r, T = T/T_r, t = tU_r/L_r, H = H/U_r^2, p = p/\rho_r U_r^2$$

This normalization leads to the following non dimensional

parameters ; Mach no., $M = U_r/c$; Prandtl no., $\mu_r c_p/k$; Reynolds no., $Re = \rho_r U_r L_r / \mu$ where c , the reference speed of sound, is defined as $c^2 = \gamma R T_r$

The fluid properties have been assumed to be constant.

Governing equations

Continuity equation

$$\frac{\partial \rho}{\partial t} + \frac{\partial \rho u_j}{\partial x_j} = 0 \quad (2.4.1)$$

Momentum equation

$$\frac{\partial \rho u_i}{\partial t} + \frac{\partial \rho u_i u_j}{\partial x_j} = - \frac{\partial p}{\partial x_i} + \frac{1}{Re} \left\{ \nabla^2 u_i + \frac{1}{3} \frac{\partial (\nabla \cdot \vec{v})}{\partial x_i} \right\} \quad (2.4.2)$$

Energy equation

$$\frac{\partial (\rho T)}{\partial t} + \frac{\partial (\rho u_j T)}{\partial x_j} = \frac{\gamma}{Re \rho r} \nabla^2 T + \gamma(\gamma-1)M^2 \left\{ \frac{1}{Re} \phi - p(\nabla \cdot \vec{v}) \right\} \quad (2.4.3)$$

where ϕ is the dissipation term given by

$$\phi = 2 \left[\left(\frac{\partial u}{\partial x} \right)^2 + \left(\frac{\partial v}{\partial y} \right)^2 + \left(\frac{\partial w}{\partial z} \right)^2 \right] + \left(\frac{\partial u}{\partial y} + \frac{\partial v}{\partial x} \right)^2 + \left(\frac{\partial v}{\partial z} + \frac{\partial w}{\partial y} \right)^2 + \left(\frac{\partial w}{\partial x} + \frac{\partial u}{\partial z} \right)^2 - \frac{2}{3} (\nabla \cdot \vec{v}) \quad (2.4.4)$$

Equation of state

$$p = \frac{\rho T}{\gamma M^2} \quad (2.4.5)$$

Boundary conditions

$$\text{plane BC'G'F} \\ u = 0 = v = w \quad (2.4.6)$$

$$\frac{\partial T}{\partial x} = 0 \quad (2.4.7)$$

$$\frac{\partial \rho}{\partial t} + \frac{\partial \rho u}{\partial x} = 0 \quad (2.4.8)$$

$$\text{Plane A'D'H'E'} \\ \frac{\partial p}{\partial x} = 0 = \frac{\partial u}{\partial x} = \frac{\partial v}{\partial x} = \frac{\partial w}{\partial x} = \frac{\partial T}{\partial x} \quad (2.4.9)$$

$$\text{Plane BA'E'F} \\ u = 0 = v = w \quad (2.4.10)$$

$$\frac{\partial T}{\partial y} = 0 \quad (2.4.11)$$

$$\frac{\partial \rho}{\partial t} + \frac{\partial \rho v}{\partial y} = 0 \quad (2.4.12)$$

Plane C'D'H'G

$$\frac{\partial p}{\partial y} = 0 = \frac{\partial u}{\partial y} = \frac{\partial v}{\partial y} = \frac{\partial w}{\partial y} = \frac{\partial T}{\partial y} \quad (2.4.13)$$

Plane A'BC'D'

$$P_{\text{stag}} = \frac{\rho T}{\gamma M^2} \left(\frac{T_{\text{stag}}}{T} \right)^{\gamma/(\gamma-1)} \quad (2.4.14)$$

$$T_{\text{stag}} = T + \frac{(\gamma-1)}{2} M^2 w^2 \quad (2.4.15)$$

$$\frac{\partial^2 w}{\partial z^2} = 0 \quad (2.4.16)$$

$$\frac{\partial u}{\partial z} = 0 = -\frac{\partial v}{\partial z} \quad (2.4.17)$$

Plane E' F G' H'

$$P_e = \frac{\rho T}{\gamma M^2} \quad (2.4.18)$$

$$\frac{\partial^2 u}{\partial z^2} = 0 = -\frac{\partial^2 v}{\partial z^2} = -\frac{\partial^2 w}{\partial z^2} = -\frac{\partial^2 T}{\partial z^2} \quad (2.4.19)$$

3. NUMERICAL METHOD

3.1 General outline

The governing equations are replaced by its implicit time difference approximations. Here backward difference scheme has been used for this approximation. Terms involving non-linearities at the implicit time level are linearized by Taylor expansion about the solution at the known time step. This results in a system of coupled differential equations which are linear for the dependent variables.

Alternating direction implicit(ADI) technique is applied to the linearized equations. There are many ways of applying ADI technique. The ADI technique developed by Douglas-Gunn[5] has been utilized here. The advantage with this ADI technique is that physical boundary conditions for the dependent variables can be used for the intermediate steps. (Appendix III)[6,7]

The equations obtained are replaced by their finite difference approximations using the standard central difference formula. When applied to successive grid points and incorporating the finite difference equations for the physical boundary conditions block-tridiagonal and tridiagonal systems of simultaneous equations are obtained which can be solved by standard block elimination methods.[2,4,5]

3.2 Finite difference equations for the governing equations

Continuity equation

Implicit time difference approximation of eqn.(2.4.1) at the unknown $(n+1)^{th}$ time step can be expressed as

$$\frac{\partial \rho}{\partial t}^{n+1} + \frac{\partial (\rho u)}{\partial x}^{n+1} + \frac{\partial (\rho v)}{\partial y}^{n+1} + \frac{\partial (\rho w)}{\partial z}^{n+1} = 0 \quad (3.2.1)$$

Using backward time difference approximation ,the above equation is written as

$$\frac{\rho^{n+1} - \rho^n}{\Delta t} + \frac{\partial(\rho u)^{n+1}}{\partial x} + \frac{\partial(\rho v)^{n+1}}{\partial y} + \frac{\partial(\rho w)^{n+1}}{\partial z} = 0 \quad (3.2.2)$$

It is convenient to work in terms of the difference of the variables at n^{th} and $(n+1)^{\text{th}}$ time steps . So eqn. (3.2.2) is written as

$$\frac{\psi^{n+1}}{\rho} + \Delta t \frac{\partial(\rho u)^{n+1}}{\partial x} + \Delta t \frac{\partial(\rho v)^{n+1}}{\partial y} + \Delta t \frac{\partial(\rho w)^{n+1}}{\partial z} = 0 \quad (3.2.3)$$

The linearization of eqn.(3.2.3) is done by Taylor expansion of non linear terms about the solution at the known time step. That is

$$\begin{aligned} (\rho u)^{n+1} &= (\rho u)^n + \rho^n \psi_u^{n+1} + u^n \psi_\rho^{n+1} + o(\Delta t^2) \\ (\rho v)^{n+1} &= (\rho v)^n + \rho^n \psi_v^{n+1} + v^n \psi_\rho^{n+1} + o(\Delta t^2) \\ (\rho w)^{n+1} &= (\rho w)^n + \rho^n \psi_w^{n+1} + w^n \psi_\rho^{n+1} + o(\Delta t^2) \end{aligned} \quad] \quad (3.2.4)$$

Making use of approximations from eqns.(3.2.4) , eqn.(3.2.3) becomes

$$\begin{aligned} \frac{\psi^{n+1}}{\rho} + \Delta t \frac{\partial}{\partial x} (\rho^n \psi_u^{n+1} + u^n \psi_\rho^{n+1}) + \Delta t \frac{\partial}{\partial y} (\rho^n \psi_v^{n+1} + v^n \psi_\rho^{n+1}) + \\ \Delta t \frac{\partial}{\partial z} (\rho^n \psi_w^{n+1} + w^n \psi_\rho^{n+1}) = - \Delta t \left\{ \frac{\partial(\rho u)^n}{\partial x} + \frac{\partial(\rho v)^n}{\partial y} + \frac{\partial(\rho w)^n}{\partial z} \right\} \end{aligned} \quad (3.2.5)$$

This gives a differential equation which is linear for the dependent variables. Now application of Douglas-Gunn ADI technique gives the following equations

$$\frac{\psi_\rho^*}{\rho} + \Delta t \frac{\partial}{\partial x} (\rho^n \psi_u^* + u^n \psi_\rho^*) = - \Delta t \left\{ \frac{\partial(\rho u)^n}{\partial x} + \frac{\partial(\rho v)^n}{\partial y} + \frac{\partial(\rho w)^n}{\partial z} \right\} \quad (3.2.6)$$

$$\psi_{\rho}^{**} + \Delta t \frac{\partial}{\partial y} (\rho^n \psi_v^{**} + v^n \psi_{\rho}^{**}) = \psi_{\rho}^* \quad (3.2.7)$$

$$\psi_{\rho}^{n+1} + \Delta t \frac{\partial}{\partial z} (\rho^n \psi_w^{n+1} + w^n \psi_{\rho}^{n+1}) = \psi_{\rho}^{**} \quad (3.2.8)$$

Finite difference approximations for the above are

$$\left(-\frac{\Delta t u_{i-1}^n}{2 \Delta x} \right) \psi_{\rho_{i-1}}^* + \psi_{\rho_i}^* + \left(\frac{\Delta t u_{i+1}^n}{2 \Delta x} \right) \psi_{\rho_{i+1}}^* + \left(-\frac{\Delta t \rho_{i-1}^n}{2 \Delta x} \right) \psi_{u_{i-1}}^* + \\ \left(\frac{\Delta t \rho_{i+1}^n}{2 \Delta x} \right) \psi_{u_{i+1}}^* = \Delta t \left\{ -\frac{\partial(\rho u)^n}{\partial x} - \frac{\partial(\rho v)^n}{\partial y} - \frac{\partial(\rho w)^n}{\partial z} \right\} \quad (3.2.9)$$

$$\left(-\frac{\Delta t v_{j-1}^n}{2 \Delta y} \right) \psi_{\rho_{j-1}}^{**} + \psi_{\rho_j}^{**} + \left(\frac{\Delta t v_{j+1}^n}{2 \Delta y} \right) \psi_{\rho_{j+1}}^{**} + \left(-\frac{\Delta t \rho_{j-1}^n}{2 \Delta y} \right) \psi_{v_{j-1}}^{**} + \\ + \left(\frac{\Delta t \rho_{j+1}^n}{2 \Delta y} \right) \psi_{v_{j+1}}^{**} = \psi_{\rho_j}^* \quad (3.2.10)$$

$$\left(-\frac{\Delta t w_{k-1}^n}{2 \Delta z} \right) \psi_{\rho_{k-1}}^{n+1} + \psi_{\rho_k}^{n+1} + \left(\frac{\Delta t w_{k+1}^n}{2 \Delta z} \right) \psi_{\rho_{k+1}}^{n+1} + \left(-\frac{\Delta t \rho_{k-1}^n}{2 \Delta z} \right) \psi_{w_{k-1}}^{n+1} + \\ + \left(\frac{\Delta t \rho_{k+1}^n}{2 \Delta z} \right) \psi_{w_{k+1}}^{n+1} = \psi_{\rho_k}^{**} \quad (3.2.11)$$

\times momentum equation

Finite difference equations are obtained by applying the steps illustrated above, with the exception that the term $\frac{\partial(\nabla \cdot \vec{V})}{\partial x}$ is evaluated at the known time step. This is done to avoid the ADI

treatment of mixed derivatives.

The finite difference equations are

$$\begin{aligned}
 & \left\{ -\frac{\Delta t}{2 \Delta x} (u^2)_{i-1}^n - \frac{\Delta t T_{i-1}^n}{2 \Delta x \gamma M^2} \right\} \psi_{\rho_{i-1}}^* + u_i^n \psi_{\rho_i}^* + \left\{ \frac{\Delta t}{2 \Delta x} (u^2)_{i+1}^n + \right. \\
 & \left. \frac{\Delta t T_{i+1}^n}{2 \Delta x \gamma M^2} \right\} \psi_{\rho_{i+1}}^* + \left(-\frac{2 \rho_{i-1}^n u_{i-1}^n \Delta t}{2 \Delta x} - \frac{\Delta t}{Re \Delta x^2} \right) \psi_{u_{i-1}}^* + \left(\rho_i^n + \right. \\
 & \left. \frac{2 \Delta t}{Re \Delta x^2} \right) \psi_{u_i}^* + \left(\frac{2 \rho_{i+1}^n u_{i+1}^n \Delta t}{2 \Delta x} - \frac{\Delta t}{Re \Delta x^2} \right) \psi_{u_{i+1}}^* + \left(-\frac{\Delta t \rho_{i-1}^n}{2 \Delta x \gamma M^2} \right) \psi_{T_{i-1}}^* \\
 & \left\{ \frac{\Delta t \rho_{i+1}^n}{2 \Delta x \gamma M^2} \right\} \psi_{T_{i+1}}^* = \Delta t \left\{ -\frac{\partial(\rho u^2)}{\partial x}^n_i - \frac{\partial(\rho u v)}{\partial y}^n_i - \frac{\partial(\rho u w)}{\partial z}^n_i - \right. \\
 & \left. \frac{1}{\gamma M^2} \frac{\partial(\rho T)}{\partial x}^n_i + \frac{1}{Re} \left(\nabla^2 u_i^n + \frac{1}{3} \frac{\partial(\nabla \cdot \vec{V})}{\partial x}^n_i \right) \right\} \quad (3.2.12)
 \end{aligned}$$

$$\begin{aligned}
 & \left\{ -\frac{\Delta t u_{j-1}^n v_{j-1}^n}{2 \Delta y} \right\} \psi_{\rho_{j-1}}^{**} + u_j^n \psi_{\rho_j}^{**} + \left\{ \frac{\Delta t u_{j+1}^n v_{j+1}^n}{2 \Delta y} \right\} \psi_{\rho_{j+1}}^{**} + \\
 & \left\{ -\frac{\Delta t \rho_{j-1}^n v_{j-1}^n}{2 \Delta y} - \frac{\Delta t}{Re \Delta y^2} \right\} \psi_{u_{j-1}}^{**} + \left(\rho_j^n + \frac{2 \Delta t}{Re \Delta y^2} z \right) \psi_{u_j}^{**} \\
 & \left\{ -\frac{\Delta t \rho_{j+1}^n v_{j+1}^n}{2 \Delta y} - \frac{\Delta t}{Re \Delta y^2} \right\} \psi_{u_{j+1}}^{**} + \left\{ -\frac{\Delta t \rho_{j-1}^n u_{j-1}^n}{2 \Delta y} \right\} \psi_{v_{j-1}}^{**} + \\
 & \left\{ \frac{\Delta t \rho_{j+1}^n u_{j+1}^n}{2 \Delta y} \right\} \psi_{v_{j+1}}^{**} = \rho_j^n \psi_{u_j}^* + u_j^n \psi_{\rho_j}^* \quad (3.2.13)
 \end{aligned}$$

$$\begin{aligned}
 & \left(-\frac{\Delta t}{2 \Delta z} u_{k-1}^n w_{k-1}^n \right) \psi_{P_{k-1}}^{n+1} + u_k^n \psi_{P_k}^{n+1} + \left(\frac{\Delta t}{2 \Delta z} u_{k+1}^n w_{k+1}^n \right) \psi_{P_{k+1}}^{n+1} + \\
 & \left(-\frac{\Delta t}{2 \Delta z} \rho_{k-1}^n w_{k-1}^n - \frac{\Delta t}{Re \Delta z^2} \right) \psi_{U_{k-1}}^{n+1} + \left(\rho_k^n + \frac{2 \Delta t}{Re \Delta z^2} \right) \psi_{U_k}^{n+1} \\
 & \left(\frac{\Delta t}{2 \Delta z} \rho_{k+1}^n w_{k+1}^n - \frac{\Delta t}{Re \Delta z^2} \right) \psi_{U_{k+1}}^{n+1} + \left(-\frac{\Delta t}{2 \Delta z} \rho_{k-1}^n u_{k-1}^n \right) \psi_{W_{k-1}}^{n+1} + \\
 & \left(\frac{\Delta t}{2 \Delta z} \rho_{k+1}^n u_{k+1}^n \right) \psi_{W_{k+1}}^{n+1} = \rho_k^n \psi_{U_k}^{**} + u_k^n \psi_{P_k}^{**}
 \end{aligned} \tag{3.2.14}$$

y momentum equation

Finite difference equations are obtained by applying the steps, illustrated above. Here the term $\frac{\partial(\nabla \cdot \vec{V})}{\partial y}$ is evaluated at the known time step.

The finite difference equations are

$$\begin{aligned}
 & \left(-\frac{\Delta t}{2 \Delta x} u_{i-1}^n v_{i-1}^n \right) \psi_{P_{i-1}}^* + v_i^n \psi_{P_i}^* + \left(\frac{\Delta t}{2 \Delta x} u_{i+1}^n v_{i+1}^n \right) \psi_{P_{i+1}}^* + \\
 & \left(-\frac{\Delta t}{2 \Delta x} \rho_{i-1}^n v_{i-1}^n \right) \psi_{U_{i-1}}^* + \left(\frac{\Delta t}{2 \Delta x} \rho_{i+1}^n v_{i+1}^n \right) \psi_{U_{i+1}}^* + \left(-\frac{\Delta t}{2 \Delta x} \rho_{i-1}^n u_{i-1}^n \right. \\
 & \left. - \frac{\Delta t}{Re \Delta x^2} \right) \psi_{V_{i-1}}^* + \left(\rho_i^n + \frac{2 \Delta t}{Re \Delta x^2} \right) \psi_{V_i}^* + \left(\frac{\Delta t}{2 \Delta x} \rho_{i+1}^n u_{i+1}^n \right. \\
 & \left. - \frac{\Delta t}{Re \Delta x^2} \right) \psi_{V_{i+1}}^* = \Delta t \left\{ -\frac{\partial(\rho u v)}{\partial x}^n_i - \frac{\partial(\rho v^2)}{\partial y}^n_i - \frac{\partial(\rho v w)}{\partial z}^n_i - \right.
 \end{aligned}$$

$$\frac{1}{\gamma M^2} \frac{\partial(\rho T)_i^n}{\partial y} + -\frac{1}{Re} \left(\nabla^2 v_i^n + -\frac{1}{3} \frac{\partial(\nabla \cdot \vec{V})_i^n}{\partial y} \right) \} \quad (3.2.15)$$

$$\begin{aligned} & \left\{ -\frac{\Delta t}{2 \Delta y} (v^2)_{j-1}^n - \frac{\Delta t T_{j-1}^n}{2 \Delta y \gamma M^2} \right\} \psi_{\rho_{j-1}}^{**} + v_j^n \psi_{\rho_j}^{**} + \left(\frac{\Delta t}{2 \Delta y} (v^2)_{j+1}^n + \right. \\ & \left. \frac{\Delta t T_{j+1}^n}{2 \Delta y \gamma M^2} \right) \psi_{\rho_{j+1}}^{**} + \left(-\frac{2 \rho_{j-1}^n v_{j-1}^n \Delta t}{2 \Delta y} - \frac{\Delta t}{Re \Delta y^2} \right) \psi_{v_{j-1}}^{**} + \left(\rho_j^n + \right. \\ & \left. \frac{2 \Delta t}{Re \Delta y^2} \right) \psi_{v_j}^{**} + \left(\frac{2 \rho_{j+1}^n u_{j+1}^n \Delta t}{2 \Delta y} - \frac{\Delta t}{Re \Delta y^2} \right) \psi_{v_{j+1}}^{**} + \left(-\frac{\Delta t \rho_{j-1}^n}{2 \Delta y \gamma M^2} \right) \psi_{T_{j-1}}^{**} \\ & + \left(\frac{\Delta t \rho_{j+1}^n}{2 \Delta y \gamma M^2} \right) \psi_{T_{j+1}}^{**} = \rho_j^n \psi_{v_j}^* + v_j^n \psi_{\rho_j}^* \end{aligned} \quad (3.2.16)$$

$$\begin{aligned} & \left(-\frac{\Delta t v_{k-1}^n w_{k-1}^n}{2 \Delta z} \right) \psi_{\rho_{k-1}}^{n+1} + v_k^n \psi_{\rho_k}^{n+1} + \left(\frac{\Delta t v_{k+1}^n w_{k+1}^n}{2 \Delta z} \right) \psi_{\rho_{k+1}}^{n+1} + \\ & \left(-\frac{\Delta t \rho_{k-1}^n w_{k-1}^n}{2 \Delta z} - \frac{\Delta t}{Re \Delta z^2} \right) \psi_{v_{k-1}}^{n+1} + \left(\rho_k^n + \frac{2 \Delta t}{Re \Delta z^2} \right) \psi_{v_k}^{n+1} \\ & \left(\frac{\Delta t \rho_{k+1}^n w_{k+1}^n}{2 \Delta z} - \frac{\Delta t}{Re \Delta z^2} \right) \psi_{v_{k+1}}^{n+1} + \left(-\frac{\Delta t \rho_{k-1}^n v_{k-1}^n}{2 \Delta z} \right) \psi_{w_{k-1}}^{n+1} + \end{aligned}$$

$$\left(\frac{\Delta t \rho_{k+1}^n v_{k+1}^n}{2 \Delta z} \right) \psi_{w_{k+1}}^{n+1} = \rho_k^n \psi_{v_k}^{**} + v_k^n \psi_{\rho_k}^{**} \quad (3.2.17)$$

z momentum equation

Here the term $\frac{\partial(\nabla \cdot \vec{V})}{\partial z}$ is evaluated at the known time step. The difference equations are

$$\left(-\frac{\Delta t}{2 \Delta x} \frac{u_{i-1}^n w_{i-1}^n}{\Delta x} \right) \psi_{P_{i-1}}^* + w_i^n \psi_{P_i}^* + \left(\frac{\Delta t}{2 \Delta x} \frac{u_{i+1}^n w_{i+1}^n}{\Delta x} \right) \psi_{P_{i+1}}^* +$$

$$\left(-\frac{\Delta t}{2 \Delta x} \frac{\rho_{i-1}^n w_{i-1}^n}{\Delta x} \right) \psi_{U_{i-1}}^* + \left(\frac{\Delta t}{2 \Delta x} \frac{\rho_{i+1}^n w_{i+1}^n}{\Delta x} \right) \psi_{U_{i+1}}^* + \left(-\frac{\Delta t}{2 \Delta x} \frac{\rho_{i-1}^n u_{i-1}^n}{\Delta x} \right)$$

$$-\frac{\Delta t}{Re \Delta x^2} \psi_{W_{i-1}}^* + \left(\rho_i^n + \frac{2 \Delta t}{Re \Delta x^2} \right) \psi_{W_i}^* + \left(\frac{\Delta t}{2 \Delta x} \frac{\rho_{i+1}^n u_{i+1}^n}{\Delta x} \right) -$$

$$\frac{\Delta t}{Re \Delta x^2} \psi_{W_{i+1}}^* = \Delta t \left\{ -\frac{\partial(\rho uw)}{\partial x}_i^n - \frac{\partial(\rho vw)}{\partial y}_i^n - \frac{\partial(\rho w^2)}{\partial z}_i^n - \frac{1}{\gamma M^2} \frac{\partial(\rho T)}{\partial z}_i^n + \frac{1}{Re} \left(\nabla^2 w_i^n + \frac{1}{3} \frac{\partial(\nabla \cdot \vec{v})}{\partial z}_i^n \right) \right\} \quad (3.2.18)$$

$$\left(-\frac{\Delta t}{2 \Delta y} \frac{v_{j-1}^n w_{j-1}^n}{\Delta y} \right) \psi_{P_{j-1}}^{**} + w_j^n \psi_{P_j}^{**} + \left(\frac{\Delta t}{2 \Delta y} \frac{v_{j+1}^n w_{j+1}^n}{\Delta y} \right) \psi_{P_{j+1}}^{**} +$$

$$\left(-\frac{\Delta t}{2 \Delta y} \frac{\rho_{j-1}^n w_{j-1}^n}{\Delta y} \right) \psi_{V_{j-1}}^{**} + \left(\frac{\Delta t}{2 \Delta y} \frac{\rho_{j+1}^n w_{j+1}^n}{\Delta y} \right) \psi_{V_{j+1}}^{**} + \left(-\frac{\Delta t}{2 \Delta y} \frac{\rho_{j-1}^n v_{j-1}^n}{\Delta y} \right)$$

$$-\frac{\Delta t}{Re \Delta y^2} \psi_{W_{j-1}}^{**} + \left(\rho_j^n + \frac{2 \Delta t}{Re \Delta y^2} \right) \psi_{W_j}^{**} + \left(\frac{\Delta t}{2 \Delta y} \frac{\rho_{j+1}^n v_{j+1}^n}{\Delta y} \right) -$$

$$\frac{\Delta t}{Re \Delta y^2} \psi_{W_{j+1}}^{**} = \rho_j^n \psi_{W_j}^* + w_j^n \psi_{P_j}^* \quad (3.2.19)$$

$$\left(-\frac{\Delta t}{2 \Delta z} \langle w^2 \rangle_{k-1}^n - \frac{\Delta t}{2 \Delta z} \frac{T_{k-1}^n}{\gamma M^2} \right) \psi_{P_{k-1}}^{n+1} + w_k^n \psi_{P_k}^{n+1} + \left(\frac{\Delta t}{2 \Delta z} \langle w^2 \rangle_{k+1}^n + \right)$$

$$\begin{aligned}
 & \left[\frac{\Delta t}{2 \Delta z} \frac{T_{k+1}^n}{\gamma M^2} \right] \psi_{P_{k+1}}^{n+1} + \left[-\frac{2 \rho_{k-1}^n w_{k-1}^n \Delta t}{2 \Delta z} - \frac{\Delta t}{Re \Delta z^2} \right] \psi_{W_{k-1}}^{n+1} + \left[\rho_k^n + \right. \\
 & \left. \frac{2 \Delta t}{Re \Delta z^2} \right] \psi_{W_k}^{n+1} + \left(\frac{2 \rho_{k+1}^n w_{k+1}^n \Delta t}{2 \Delta z} - \frac{\Delta t}{Re \Delta z^2} \right) \psi_{W_{k+1}}^{n+1} + \left(-\frac{\Delta t \rho_{k-1}^n}{2 \Delta z \gamma M^2} \right) \psi_{T_{k-1}}^{n+1} \\
 & + \left(\frac{\Delta t \rho_{k+1}^n}{2 \Delta z \gamma M^2} \right) \psi_{T_{k+1}}^{n+1} = \rho_k^n \psi_{W_k}^{**} + w_k^n \psi_{P_k}^{**} \quad (3.2.20)
 \end{aligned}$$

Energy equation

While obtaining the finite difference equations for the energy equation, the diffusion term ϕ is evaluated at the known time step. This is done to avoid, the finite difference equations, from getting much complicated.

$$\begin{aligned}
 & \left(-\frac{\Delta t}{2 \Delta x} u_{i-1}^n T_{i-1}^n \right) \psi_{P_{i-1}}^* + \left(T_i^n + \Delta t(\gamma-1) \left(\frac{\partial u}{\partial x} \right)_i^n T_i^n \right) \psi_{P_i}^* + \\
 & \left(\frac{\Delta t}{2 \Delta x} u_{i+1}^n T_{i+1}^n \right) \psi_{P_{i+1}}^* + \left(-\frac{\Delta t}{2 \Delta x} \rho_{i-1}^n T_{i-1}^n - \frac{\Delta t(\gamma-1)}{2 \Delta x} \rho_i^n T_i^n \right) \psi_{U_{i-1}}^* \\
 & + \left(\frac{\Delta t}{2 \Delta x} \rho_{i+1}^n T_{i+1}^n + \frac{\Delta t(\gamma-1)}{2 \Delta x} \rho_i^n T_i^n \right) \psi_{U_{i+1}}^* + \left(-\frac{\Delta t}{2 \Delta x} \rho_{i-1}^n u_{i-1}^n - \right. \\
 & \left. \frac{\gamma \Delta t}{Re \Pr \Delta x^2} \right) \psi_{T_{i-1}}^* + \left(\rho_i^n + \Delta t(\gamma-1) \left(\frac{\partial u}{\partial x} \right)_i^n \rho_i^n + \frac{2 \gamma \Delta t}{Re \Pr \Delta x^2} \right) \psi_{T_i}^* + \\
 & \left(\frac{\Delta t}{2 \Delta x} \rho_{i+1}^n u_{i+1}^n - \frac{\gamma \Delta t}{Re \Pr \Delta x^2} \right) \psi_{T_{i+1}}^* = \Delta t \left\{ -\frac{\partial (\rho u T)}{\partial x} \right|_i^n - \frac{\partial (\rho v T)}{\partial y} \right|_i^n -
 \end{aligned}$$

$$\frac{\partial(\rho_w T)}{\partial z}^n_i - (\gamma-1) \rho_i^n T_i^n (\nabla \cdot \vec{V})_i^n + \frac{\gamma}{Re \ Pr} (\nabla^2 T)_i^n + \frac{\gamma(\gamma-1) M^2}{Re} \phi_i^n \quad \{$$

(3.2.21)

$$\begin{aligned} & \left[-\frac{\Delta t}{2 \Delta y} v_{j-1}^n T_{j-1}^n \right] \psi_{\rho_{j-1}}^{**} + \left[T_j^n + \Delta t(\gamma-1) \left(\frac{\partial v}{\partial y} \right)_j^n T_j^n \right] \psi_{\rho_j}^{**} + \\ & \left[\frac{\Delta t}{2 \Delta y} v_{j+1}^n T_{j+1}^n \right] \psi_{\rho_{j+1}}^{**} + \left[-\frac{\Delta t}{2 \Delta y} \rho_{j-1}^n T_{j-1}^n - \frac{\Delta t(\gamma-1)}{2 \Delta y} \rho_j^n T_j^n \right] \psi_{v_{j-1}}^{**} + \\ & + \left[\frac{\Delta t}{2 \Delta y} \rho_{j+1}^n T_{j+1}^n + \frac{\Delta t(\gamma-1)}{2 \Delta y} \rho_j^n T_j^n \right] \psi_{v_{j+1}}^{**} + \left[-\frac{\Delta t}{2 \Delta y} \rho_{j-1}^n v_{j-1}^n - \right. \\ & \left. \frac{\gamma \Delta t}{Re \ Pr \ Delta y^2} \right] \psi_{T_{j-1}}^{**} + \left[\rho_j^n + \Delta t(\gamma-1) \left(\frac{\partial v}{\partial y} \right)_j^n \rho_j^n + \frac{2 \gamma \Delta t}{Re \ Pr \ Delta y^2} \right] \psi_{T_j}^{**} + \\ & \left[\frac{\Delta t}{2 \Delta y} \rho_{j+1}^n u_{j+1}^n - \frac{\gamma \Delta t}{Re \ Pr \ Delta y^2} \right] \psi_{T_{j+1}}^{**} = \rho_j^n \psi_{T_j}^* + T_j^n \psi_{\rho_j}^* \quad (3.2.22) \end{aligned}$$

$$\begin{aligned} & \left[-\frac{\Delta t}{2 \Delta z} w_{k-1}^n T_{k-1}^n \right] \psi_{\rho_{k-1}}^{n+1} + \left[T_k^n + \Delta t(\gamma-1) \left(\frac{\partial w}{\partial z} \right)_k^n T_k^n \right] \psi_{\rho_k}^{n+1} + \\ & \left[\frac{\Delta t}{2 \Delta z} w_{k+1}^n T_{k+1}^n \right] \psi_{\rho_{k+1}}^{n+1} + \left[-\frac{\Delta t}{2 \Delta z} \rho_{k-1}^n T_{k-1}^n - \frac{\Delta t(\gamma-1)}{2 \Delta z} \rho_k^n T_k^n \right] \psi_{w_{k-1}}^{n+1} + \\ & + \left[\frac{\Delta t}{2 \Delta z} \rho_{k+1}^n T_{k+1}^n + \frac{\Delta t(\gamma-1)}{2 \Delta z} \rho_k^n T_k^n \right] \psi_{w_{k+1}}^{n+1} + \left[-\frac{\Delta t}{2 \Delta z} \rho_{k-1}^n w_{k-1}^n - \right. \\ & \left. \frac{\gamma \Delta t}{Re \ Pr \ Delta z^2} \right] \psi_{T_{k-1}}^{n+1} + \left[\rho_k^n + \Delta t(\gamma-1) \left(\frac{\partial w}{\partial z} \right)_k^n \rho_k^n + \frac{2 \gamma \Delta t}{Re \ Pr \ Delta z^2} \right] \psi_{T_k}^{n+1} + \end{aligned}$$

$$\left(\frac{\Delta t}{2 \Delta z} \rho_{k+1}^n w_{k+1}^n - \frac{\gamma \Delta t}{Re \ Pr \ \Delta z^2} \right) \psi_{T_{k+1}}^{n+1} = \rho_k^n \psi_{T_k}^{**} + T_k^n \psi_{\rho_k}^{**} \quad (3.2.23)$$

3.3 Finite difference equations for the boundary conditions

For obtaining the finite difference equations for the boundary conditions, the steps, which have been already followed for the governing equations, are applied. Three point, one sided,

difference approximations are used for the boundary conditions.

Plane B C' G' F

Finite difference approximations for eqns.(2.4.6) are

$$\psi_{u_{i=0}}^{n+1} = 0 = \psi_{v_0}^{n+1} = \psi_{w_0}^{n+1} \quad (3.3.1)$$

Finite difference approximation for the equation (2.4.7) is

$$3 \psi_{T_{i=0}}^{n+1} - 4 \psi_{T_1}^{n+1} + \psi_{T_2}^{n+1} = 0 \quad (3.3.2)$$

Density is determined from the equation (2.4.8). Implicit time difference approximation of this equation is

$$\begin{aligned} \frac{\partial \rho^{n+1}}{\partial t} + \frac{\partial (\rho u)^{n+1}}{\partial x} &= 0 \\ \Rightarrow \psi_{\rho}^{n+1} + \Delta t \frac{\partial (\rho u)^{n+1}}{\partial x} &= 0 \end{aligned}$$

Linearization followed by space differencing of the above equation gives

$$\begin{aligned} \left(1 - \frac{3 \Delta t}{2 \Delta x} u_{i=0}^n \right) \psi_{\rho_{i=0}}^{n+1} + \left(\frac{4 \Delta t}{2 \Delta x} u_1^n \right) \psi_{\rho_1}^{n+1} + \left(- \frac{\Delta t}{2 \Delta x} u_2^n \right) \psi_{\rho_2}^{n+1} + \\ \left(- \frac{3 \Delta t}{2 \Delta x} \rho_0^n \right) \psi_{u_0}^{n+1} + \left(\frac{4 \Delta t}{2 \Delta x} \rho_1^n \right) \psi_{u_1}^{n+1} + \left(- \frac{\Delta t}{2 \Delta x} \rho_2^n \right) \psi_{u_2}^{n+1} &= \end{aligned}$$

$$- \Delta t \frac{\partial(\rho u)}{\partial x} \Big|_o^n \quad (3.3.3)$$

Plane A' D' H' E'

Finite difference approximations for the equation (2.4.9) are

$$\psi_{\rho_{i=L-2}}^{n+1} - 4 \psi_{\rho_{L-1}}^{n+1} + 3 \psi_{\rho_L}^{n+1} = - \rho_{L-2}^n + 4\rho_{L-1}^n - 3\rho_L^n \quad (3.3.4)$$

$$\psi_{u_{i=L-2}}^{n+1} - 4 \psi_{u_{L-1}}^{n+1} + 3 \psi_{u_L}^{n+1} = - u_{L-2}^n + 4u_{L-1}^n - 3u_L^n \quad (3.3.5)$$

$$\psi_{v_{i=L-2}}^{n+1} - 4 \psi_{v_{L-1}}^{n+1} + 3 \psi_{v_L}^{n+1} = - v_{L-2}^n + 4v_{L-1}^n - 3v_L^n \quad (3.3.6)$$

$$\psi_{w_{i=L-2}}^{n+1} - 4 \psi_{w_{L-1}}^{n+1} + 3 \psi_{w_L}^{n+1} = - w_{L-2}^n + 4w_{L-1}^n - 3w_L^n \quad (3.3.7)$$

$$\psi_{T_{i=L-2}}^{n+1} - 4 \psi_{T_{L-1}}^{n+1} + 3 \psi_{T_L}^{n+1} = - T_{L-2}^n + 4T_{L-1}^n - 3T_L^n \quad (3.3.8)$$

Plane B A' E' F

Finite difference approximations for eqns.(2.4.10) are

$$\psi_{u_j=0}^{n+1} = 0 = \psi_{v_o}^{n+1} = \psi_{w_o}^{n+1} \quad (3.3.9)$$

Finite difference approximation for the equation (2.4.11) is

$$3 \psi_{T_{j=0}}^{n+1} - 4 \psi_{T_1}^{n+1} + \psi_{T_2}^{n+1} = 0 \quad (3.3.10)$$

Density is determined from the equation (2.4.12). Implicit time difference for the equation (2.4.12) is

$$\frac{\rho^{n+1} - \rho^n}{\Delta t} + \frac{\partial(\rho v)}{\partial y}^{n+1} = 0$$

$$\rightarrow \psi_{\rho}^{n+1} + \Delta t \frac{\partial(\rho v)}{\partial y}^{n+1} = 0$$

Linearization followed by space differencing of the above equation gives

$$\left(1 - \frac{3}{2} \frac{\Delta t}{\Delta y} v_{j=0}^n \right) \psi_{\rho_{j=0}}^{n+1} + \left(\frac{4}{2} \frac{\Delta t}{\Delta y} v_1^n \right) \psi_{\rho_1}^{n+1} + \left(- \frac{1}{2} \frac{\Delta t}{\Delta y} v_2^n \right) \psi_{\rho_2}^{n+1} + \\ \left(- \frac{3}{2} \frac{\Delta t}{\Delta y} \rho_0^n \right) \psi_{v_0}^{n+1} + \left(\frac{4}{2} \frac{\Delta t}{\Delta y} \rho_1^n \right) \psi_{v_1}^{n+1} + \left(- \frac{1}{2} \frac{\Delta t}{\Delta y} \rho_2^n \right) \psi_{v_2}^{n+1} = \\ - \Delta t \frac{\partial(\rho v)}{\partial y} \Big|_0^n \quad (3.3.11)$$

Plane C' G' H' D'

Finite difference approximations for the equation (2.4.13) are

$$\psi_{\rho_{j=M-2}}^{n+1} - 4 \psi_{\rho_{M-1}}^{n+1} + 3 \psi_{\rho_M}^{n+1} = - \rho_{M-2}^n + 4 \rho_{M-1}^n - 3 \rho_M^n \quad (3.3.12)$$

$$\psi_{u_{j=M-2}}^{n+1} - 4 \psi_{u_{M-1}}^{n+1} + 3 \psi_{u_M}^{n+1} = - u_{M-2}^n + 4 u_{M-1}^n - 3 u_M^n \quad (3.3.13)$$

$$\psi_{v_{j=M-2}}^{n+1} - 4 \psi_{v_{M-1}}^{n+1} + 3 \psi_{v_M}^{n+1} = - v_{M-2}^n + 4 v_{M-1}^n - 3 v_M^n \quad (3.3.14)$$

$$\psi_{w_{j=M-2}}^{n+1} - 4 \psi_{w_{M-1}}^{n+1} + 3 \psi_{w_M}^{n+1} = - w_{M-2}^n + 4 w_{M-1}^n - 3 w_M^n \quad (3.3.15)$$

$$\psi_{T_{j=M-2}}^{n+1} - 4 \psi_{T_{M-1}}^{n+1} + 3 \psi_{T_M}^{n+1} = - T_{M-2}^n + 4 T_{M-1}^n - 3 T_M^n \quad (3.3.16)$$

Plane A' B C' D'

From equation (2.4.15)

$$P_{stag} = \frac{\rho^{n+1} T^{n+1}}{\gamma M^2} \left(\frac{T^{n+1}}{T_{stag}} \right)^{\gamma/(\gamma-1)} = \frac{\rho^n T^n}{\gamma M^2} \left(\frac{T^n}{T_{stag}} \right)^{\gamma/(\gamma-1)}$$

Linearization followed by finite difference approximation of the above equation gives

$$\psi_{\rho_{k=0}}^{n+1} + \frac{1}{(1-\gamma)} \frac{\rho_{k=0}^n}{T_{k=0}^n} \psi_{T_{k=0}}^{n+1} = 0 \quad (3.3.17)$$

From equation (2.4.15)

$$T_{\text{stag}} = T^{n+1} + \frac{(\gamma - 1)}{2} M^2 (w^2)^{n+1} = T^n + \frac{(\gamma - 1)}{2} M^2 (w^2)^n$$

Linearization followed by finite difference approximation of the above equation gives

$$(\gamma - 1) M^2 w_{k=0}^n \psi_{w_{k=0}}^{n+1} + \psi_{T_{k=0}}^{n+1} = 0 \quad (3.3.18)$$

Finite difference approximation for the equation (2.4.16) is

$$\psi_{w_{k=0}}^{n+1} - 2 \psi_{w_1}^{n+1} + \psi_{w_2}^{n+1} = - w_0^n + 2w_1^n - w_2^n \quad (3.3.19)$$

Finite difference approximations for the equation (2.4.17) are

$$3 \psi_{u_{k=0}}^{n+1} - 4 \psi_{u_1}^{n+1} + \psi_{u_2}^{n+1} = - 3u_0^n + 4u_1^n - u_2^n \quad (3.3.20)$$

$$3 \psi_{v_{k=0}}^{n+1} - 4 \psi_{v_1}^{n+1} + \psi_{v_2}^{n+1} = - 3v_0^n + 4v_1^n - v_2^n \quad (3.3.21)$$

Plane E'F G'H'

From equation (2.4.18)

$$P_{\text{static}} = \frac{(\rho T)^{n+1}}{\gamma M^2} = \frac{(\rho T)^n}{\gamma M^2}$$

Linearization followed by finite difference approximation of the above equation gives

$$T^n \psi_{P_{k=N}}^{n+1} + \rho^n \psi_{T_N}^{n+1} = 0 \quad (3.3.22)$$

Finite difference approximations for the equation are

$$\psi_{u_{k=N-2}}^{n+1} - 2 \psi_{u_{N-1}}^{n+1} + \psi_{u_N}^{n+1} = - u_{N-2}^n + 2u_{N-1}^n - u_N^n \quad (3.3.23)$$

$$\psi_{v_{k=N-2}}^{n+1} - 2\psi_{v_{N-1}}^{n+1} + \psi_{v_N}^{n+1} = -v_{N-2}^n + 2v_{N-1}^n - v_N^n \quad (3.3.24)$$

$$\psi_{w_{k=N-2}}^{n+1} - 2\psi_{w_{N-1}}^{n+1} + \psi_{w_N}^{n+1} = -w_{N-2}^n + 2w_{N-1}^n - w_N^n \quad (3.3.25)$$

$$\psi_{T_{k=N-2}}^{n+1} - 2\psi_{T_{N-1}}^{n+1} + \psi_{T_N}^{n+1} = -T_{N-2}^n + 2T_{N-1}^n - T_N^n \quad (3.3.26)$$

3.4 Solution procedure for the finite difference equations

Careful study of the difference equations reveals that, for each ADI step, it is required to solve one block-tridiagonal system of equations and two simple tridiagonal systems of equations.

During the first step of the ADI procedure (ie.marching along x axis), only the derivatives with respect to x and t appear in the implicit difference equations.In the continuity, x momentum and energy equations, these implicitly treated terms contain ρ , u and T ,but not v and w .Therefore the difference equations from these three equations can be solved for ρ^* , u^* , and T^* .Having obtained the values of ρ^* , u^* , and T^* the difference equations for y and z momentum equations can be solved independently for v^* and w^* since y and z momentum equations are uncoupled with respect to v^* and w^* .Solution of v^* requires the solution of simple tridiagonal system of equations.Similarly solution of w^* also requires the solution of simple tridiagonal system of equations.This special nature of coupling improves the computational efficiency.

During the second ADI step (ie. marching along y axis) the difference equations from the continuity , y momentum and energy equations are solved as coupled equations for ρ^{**} , v^{**} ,and T^{**} . Having obtained the values of ρ^{**} , v^{**} ,and T^{**} the difference equations for x and z momentum equations can be solved

independently for u^{**} and w^{**} since x and z momentum equations are uncoupled with respect to u^{**} and w^{**} .

During the third ADI step (ie. marching along z axis) the difference equations from continuity, z momentum and energy equations are solved as coupled equations for ρ^{n+1}, w^{n+1} , and T^{n+1} and difference equations for x and y momentum equations can be solved independently for u^{n+1} and v^{n+1} .

First ADI step

From equations (3.2.9), (3.2.12), (3.2.21) and (3.3.1), (3.3.2), (3.3.3) the following system of equations is obtained

$$\begin{bmatrix} A_0 & C_0 & E \\ B_1 & A_1 & C_1 \\ B_2 & A_2 & C_2 \\ 0 & F_L & B_L & A_L \end{bmatrix} \begin{Bmatrix} \psi_0^* \\ \psi_1^* \\ \psi_2^* \\ \psi_L^* \end{Bmatrix} = \begin{Bmatrix} R_0 \\ R_1 \\ R_2 \\ R_L \end{Bmatrix} \quad (3.4.1)$$

where

$$A_0 = \begin{bmatrix} 1 - \frac{3 \Delta t}{2 \Delta x} u_{i=0}^n & -\frac{3 \Delta t}{2 \Delta x} \rho_0^n & 0 \\ 0 & 1 & 0 \\ 0 & 0 & 3 \end{bmatrix}$$

$$C_0 = \begin{bmatrix} \frac{4 \Delta t}{2 \Delta x} u_{i=1}^n & \frac{4 \Delta t}{2 \Delta x} \rho_1^n & 0 \\ 0 & 0 & 0 \\ 0 & 0 & -4 \end{bmatrix}$$

$$\mathbb{E} = \begin{bmatrix} -\frac{\Delta t}{2 \Delta x} u_{i=2}^n & -\frac{\Delta t}{2 \Delta x} \rho_2^n & 0 \\ 0 & 0 & 0 \\ 0 & 0 & 1 \end{bmatrix}$$

$$\mathbb{R}_0 = \left\{ \begin{array}{l} -\Delta t \frac{\partial(\rho u)}{\partial x}^n_0 \\ 0 \\ \vdots \\ -3T_0^n + 4T_1^n - T_2^n \end{array} \right\}$$

For $0 < i < L$

$$\mathbb{B}_i = \begin{bmatrix} -\frac{\Delta t u_{i-1}^n}{2 \Delta x} & -\frac{\Delta t \rho_{i-1}^n}{2 \Delta x} & 0 \\ -\frac{\Delta t}{2 \Delta x} (u^2)_{i-1}^n & -\frac{2 \rho_{i-1}^n u_{i-1}^n \Delta t}{2 \Delta x} - \frac{\Delta t}{Re \Delta x^2} & -\frac{\Delta t \rho_{i-1}^n}{2 \Delta x \gamma M^2} \\ \frac{\Delta t T_{i-1}^n}{2 \Delta x \gamma M^2} & -\frac{\Delta t}{2 \Delta x} \rho_{i-1}^n T_{i-1}^n & -\frac{\Delta t}{2 \Delta x} \rho_{i-1}^n u_{i-1}^n \\ -\frac{\Delta t u_{i-1}^n T_{i-1}^n}{2 \Delta x} & \frac{\Delta t (\gamma-1)}{2 \Delta x} \rho_i^n T_i^n & -\frac{\gamma \Delta t}{Re pr \Delta x^2} \end{bmatrix}$$

$$\mathbb{A}_i = \begin{bmatrix} 1 & 0 & 0 \\ u_i^n & \rho_i^n + \frac{2 \Delta t}{Re \Delta x^2} & 0 \\ T_i^n + \Delta t (\gamma-1) \left(\frac{\partial u}{\partial x} \right)_i^n T_i^n & 0 & \rho_i^n + \Delta t (\gamma-1) \left(\frac{\partial u}{\partial x} \right)_i^n \rho_i^n \\ & & + \frac{2 \gamma \Delta t}{Re pr \Delta x^2} \end{bmatrix}$$

$$\mathbf{C}_i = \begin{bmatrix} \frac{\Delta t u_{i+1}^n}{2 \Delta x} & \frac{\Delta t \rho_{i+1}^n}{2 \Delta x} & 0 \\ \frac{\Delta t}{2 \Delta x} (u^2)_{i+1}^n + \frac{\Delta t T_{i+1}^n}{2 \Delta x \gamma M^2} & \frac{2 \rho_{i+1}^n u_{i+1}^n \Delta t}{2 \Delta x} - \frac{\Delta t}{Re \Delta x^2} & \frac{\Delta t \rho_{i+1}^n}{2 \Delta x \gamma M^2} \\ \frac{\Delta t u_{i+1}^n T_{i+1}^n}{2 \Delta x} & \frac{\Delta t (\gamma-1)}{2 \Delta x} \rho_i^n T_i^n & - \frac{\gamma \Delta t}{Re pr \Delta x^2} \end{bmatrix}$$

$$\mathbf{R}_i = \begin{bmatrix} \Delta t \left\{ - \frac{\partial(\rho u)^n}{\partial x} - \frac{\partial(\rho v)^n}{\partial y} - \frac{\partial(\rho w)^n}{\partial z} \right\} \\ \Delta t \left\{ - \frac{\partial(\rho u^2)_i^n}{\partial x} - \frac{\partial(\rho uv)_i^n}{\partial y} - \frac{\partial(\rho uw)_i^n}{\partial z} - \frac{1}{\gamma M^2} \frac{\partial(\rho T)_i^n}{\partial x} + \frac{1}{Re} \left(\nabla^2 u_i^n + \frac{1}{3} \frac{\partial(\nabla \cdot \vec{V})_i^n}{\partial x} \right) \right\} \\ \Delta t \left\{ - \frac{\partial(\rho u T)_i^n}{\partial x} - \frac{\partial(\rho v T)_i^n}{\partial y} - \frac{\partial(\rho w T)_i^n}{\partial z} - (\gamma-1) \rho_i^n T_i^n (\nabla \cdot \vec{V})_i^n + \frac{\gamma}{Re pr} (\nabla^2 T)_i^n + \frac{\gamma(\gamma-1)M^2}{Re} \phi_i^n \right\} \end{bmatrix}$$

$$\mathbf{F} = \begin{bmatrix} 1 & 0 & 0 \\ 0 & 1 & 0 \\ 0 & 0 & 1 \end{bmatrix} \quad \mathbf{B}_L = \begin{bmatrix} -4 & 0 & 0 \\ 0 & -4 & 0 \\ 0 & 0 & -4 \end{bmatrix}$$

$$A_L = \begin{bmatrix} 3 & 0 & 0 \\ 0 & 3 & 0 \\ 0 & 0 & 3 \end{bmatrix} \quad R_L = \begin{Bmatrix} -\rho_{L-2}^n + 4\rho_{L-1}^n - 3\rho_L^n \\ -u_{L-2}^n + 4u_{L-1}^n - 3u_L^n \\ -T_{L-2}^n + 4T_{L-1}^n - 3T_L^n \end{Bmatrix}$$

The system of equations (3.4.1) gives the values of ρ^* , u^* and T^* at all the grid points except for $j = 0, M$ and $k = 0, N$, for which the values are calculated directly from the boundary conditions. Equations (3.2.15), (3.3.1) and (3.3.7) give a system of equations represented as

$$\begin{bmatrix} d_0 & a_0 & e \\ b_1 & d_1 & a_1 \\ b_2 & d_2 & a_2 \\ \vdots & & \\ 0 & f & b_L & d_L \end{bmatrix} \begin{Bmatrix} \psi_v^* \\ \psi_v^* \\ \psi_v^* \\ \vdots \\ \psi_v^* \end{Bmatrix} = \begin{Bmatrix} r_0 \\ r_1 \\ r_2 \\ \vdots \\ r_L \end{Bmatrix} \quad (3.4.2)$$

where $d_0 = 1$, $a_0 = 0$, $e = 0$, $r_0 = 0$

for $i = 1$ to $(L - 1)$

$$b_i = -\frac{\Delta t}{2 \Delta x} \rho_{i-1}^n u_{i-1}^n - \frac{\Delta t}{Re \Delta x^2}$$

$$d_i = \rho_i^n + \frac{2 \Delta t}{Re \Delta x^2}$$

$$a_i = \frac{\Delta t}{2 \Delta x} \rho_{i+1}^n u_{i+1}^n - \frac{\Delta t}{Re \Delta x^2}$$

$$\begin{aligned}
 r_i = & \Delta t \left\{ -\frac{\partial(\rho uv)^n}{\partial x}_i - \frac{\partial(\rho v^2)^n}{\partial y}_i - \frac{\partial(\rho vw)^n}{\partial z}_i - \frac{1}{\gamma M^2} \frac{\partial(\rho T)^n}{\partial y}_i + \right. \\
 & \left. \frac{1}{Re} \left(\nabla^2 v^n_i + \frac{1}{3} \frac{\partial(\nabla \cdot \vec{V})^n}{\partial y}_i \right) \right\} + \left(\frac{\Delta t}{2 \Delta x} u^n_{i-1} v^n_{i-1} \right) \psi_{\rho_{i-1}}^* - v^n_i \psi_{\rho_i}^* \\
 - & \left(\frac{\Delta t}{2 \Delta x} u^n_{i+1} v^n_{i+1} \right) \psi_{\rho_{i+1}}^* + \left(\frac{\Delta t}{2 \Delta x} \rho^n_{i-1} v^n_{i-1} \right) \psi_{u_{i-1}}^* + \\
 & \left(- \frac{\Delta t}{2 \Delta x} \rho^n_{i+1} v^n_{i+1} \right) \psi_{u_{i+1}}^*
 \end{aligned}$$

$$f = 1, b_L = -4, d_L = 3, r_L = -v^n_{L-2} + 4v^n_{L-1} - 3v^n_L$$

System of equations (3.4.2) gives the values of v^* at all the grid points except for $j = 0, M$ and $k = 0, N$ for which the values are calculated directly from the boundary conditions.

Similarly equations (3.2.18), (3.3.1) and (3.3.7) give a system of equations similar to (3.4.2). Application of boundary conditions gives the values of w^* at all the grid points.

Second ADI step

Here equations (3.2.10), (3.2.16), (3.2.22) along with equations (3.3.9), (3.3.10), (3.3.11), (3.3.12), (3.3.14), (3.3.16) gives a system of equations of the form (3.4.1).

Equation (3.2.13) along with equations (3.3.9) and (3.3.13) gives a system of equations of the form (3.4.2).

Equation (3.2.19) along with equations (3.3.9) and (3.3.15) gives a system of equations of the form (3.4.2).

Thus the values of $\rho^{**}, u^{**}, v^{**}, w^{**}, T^{**}$ are calculated at all the grid points except $i = 0, L$ and $k = 0, N$, for which the values are calculated directly from the boundary conditions.

Third ADI step

Here equations (3.2.11), (3.2.20), (3.2.23) along with equations (3.3.17), (3.3.18), (3.3.19), (3.3.22), (3.3.25), (3.3.26) gives a system of equations of the form (3.4.1).

Equation (3.2.14) along with equations (3.3.20) and (3.3.23) gives a system of equations of the form (3.4.2).

Equation (3.2.17) along with equations (3.3.21) and (3.3.24) gives a system of equations of the form (3.4.2).

Thus the values of $\rho^{n+1}, u^{n+1}, v^{n+1}, w^{n+1}, T^{n+1}$ are calculated at all the grid points except $i = 0, L$ and $j = 0, M$, for which the values are calculated directly from the boundary conditions.

3.5 Tridiagonal form

Systems of equations (3.4.1) and (3.4.2) may be easily reduced to block-tridiagonal and tridiagonal systems of equations respectively. This is done so that standard algorithms may be applied to solve the system of equations. This increases the computational efficiency. (Appendix I and Appendix II)

System of equation (3.4.1) is reduced to block-tridiagonal form if the matrices E and F can be eliminated. E is eliminated in the following manner.

$$A_0 \psi_0^* + C_0 \psi_1^* + E \psi_2^* = R_0 \quad (3.4.3a)$$

$$B_1 \psi_0^* + A_1 \psi_1^* + C_1 \psi_2^* = R_1 \quad (3.4.3b)$$

Multiplying equation (3.4.3b) by $E C_1^{-1}$ and then subtracting it from equation gives

$$(A_0 - E C_1^{-1} B_1) \psi_0^* + (C_0 - E C_1^{-1} A_1) \psi_1^* = (R_0 - E C_1^{-1} R_1)$$

Therefore if E has to be eliminated A_o , C_o , and R_o are transformed as follows

$$A'_o = A_o - E C_1^{-1} B_1$$

$$C'_o = C_o - E C_1^{-1} A_1$$

$$R'_o = R_o - E C_1^{-1} R_1$$

A'_o , C'_o , R'_o being the transformed values of A_o , C_o , R_o .

Similarly B_L , A_L , R_L are transformed to eliminate F .

System of equations (3.4.2) is reduced to tridiagonal form if e and f are eliminated. e is eliminated in the following manner.

$$d_o \psi_{v_o}^* + a_o \psi_{v_1}^* + e \psi_{v_2}^* = r_o \quad (3.4.4a)$$

$$b_1 \psi_{v_o}^* + d_1 \psi_{v_1}^* + a_1 \psi_{v_2}^* = r_1 \quad (3.4.4b)$$

Multiplying (3.4.4b) by $\frac{e}{a_1}$ and then subtracting it from (3.4.4a) gives

$$\left(d_o - \frac{b_1}{a_1} e \right) \psi_{v_o}^* + \left(a_o - \frac{d_1}{a_1} e \right) \psi_{v_1}^* = r_o - \frac{r_1}{a_1} e$$

Therefore if e has to be eliminated then d_o , a_o and r_o are transformed as follows

$$d'_o = d_o - \frac{b_1}{a_1} e, \quad a'_o = a_o - \frac{d_1}{a_1} e, \quad r'_o = r_o - \frac{r_1}{a_1} e$$

where d'_o , a'_o and r'_o are the transformed values of d_o , a_o and r_o respectively.

3.6 Initial conditions

Uniform flow in the axial direction has been assumed as the initial condition. No slip conditions have been applied, where

applicable. Linear variation of density along axial direction has been taken.

Stagnation pressure and stagnation temperature are specified and downstream static pressure is impulsively reduced to its specified value. The duct geometry has been taken as $x_1 = l = y_1$; $z_1 = 0.5$.

5. RESULT AND DISCUSSIONS

The numerical scheme, as described in previous chapter, has been implemented, with the help of computer, to solve the flow field through a rectangular duct, fed through a stagnant reservoir of fluid at one end and a specified pressure at the downstream end. The primary aim is to predict the detailed compressible, three-dimensional flow field to establish the validity of the computer code developed. The computer code developed may be used for solving flow fields in intakes and in solid rocket thrust chambers. Computations have been done by varying the input parameters to determine their effect on the flow field as well as the limitations of the method, if any.

EFFECT OF DIFFERENT PARAMETERS

Figures 4.1 and 4.2 show the variation of axial velocity (w), with w at a fixed value of y at the upstream and downstream ends for a certain values of input parameters viz. p_{stag} , T_{stag} , P_e , Re and M . These curves indicate the typical characteristics of boundary layer profile. Also there occurs thickening of the boundary layers in the downstream direction. This suggests that the flow is developing.

The variations of centreline axial velocity and pressure along axial direction are shown in figures 4.3 and 4.4 respectively. The flow is found to be accelerating.

In figures 4.5 and 4.6 variations of centreline velocity and centreline pressure respectively have been shown for a higher value of p_e . Also centreline velocity is less for higher p_e .

Figures 4.7, 4.8 and figures 4.9, 4.10 show the effect of p_{stag} on the flow field.

figures 4.11, 4.12, 4.13, 4.14 and figures 4.15, 4.16, 4.17, 4.18, show the effect of Re on the flow field. It is observed that higher the Re, lesser is the boundary layer thickness.

Figures 4.19, 4.20 and figures 4.21, 4.22 show the effect of Mach number on the flow field.

Effect of mesh size

Different mesh sizes were used to compute the results. It is seen that the solutions are in satisfactory agreement. However the computer time increases considerably for finer mesh sizes. System time increases from around 4 seconds for $6 \times 6 \times 6$ grid to around 30 seconds for $6 \times 6 \times 21$ grid. The system times are for 'tsrx'. Here it is noteworthy that system times are higher for higher values of Re.

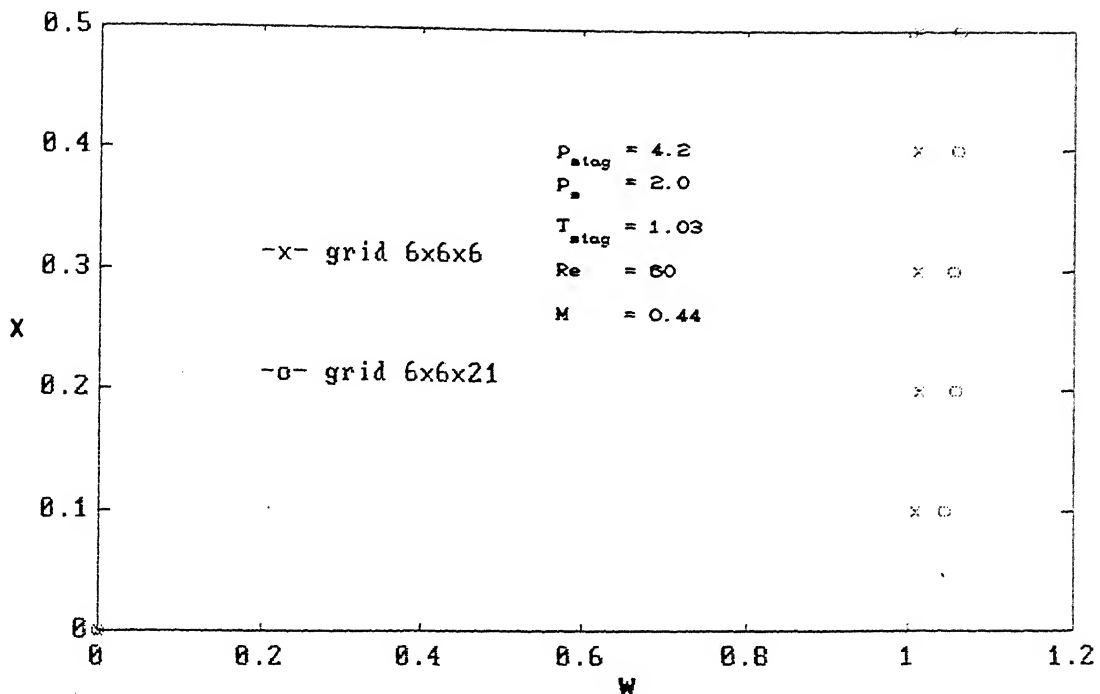


FIG 4.1 VARIATION OF COMPUTED AXIAL VELOCITY ALONG X
AT $Y = 0.5, Z = 0$

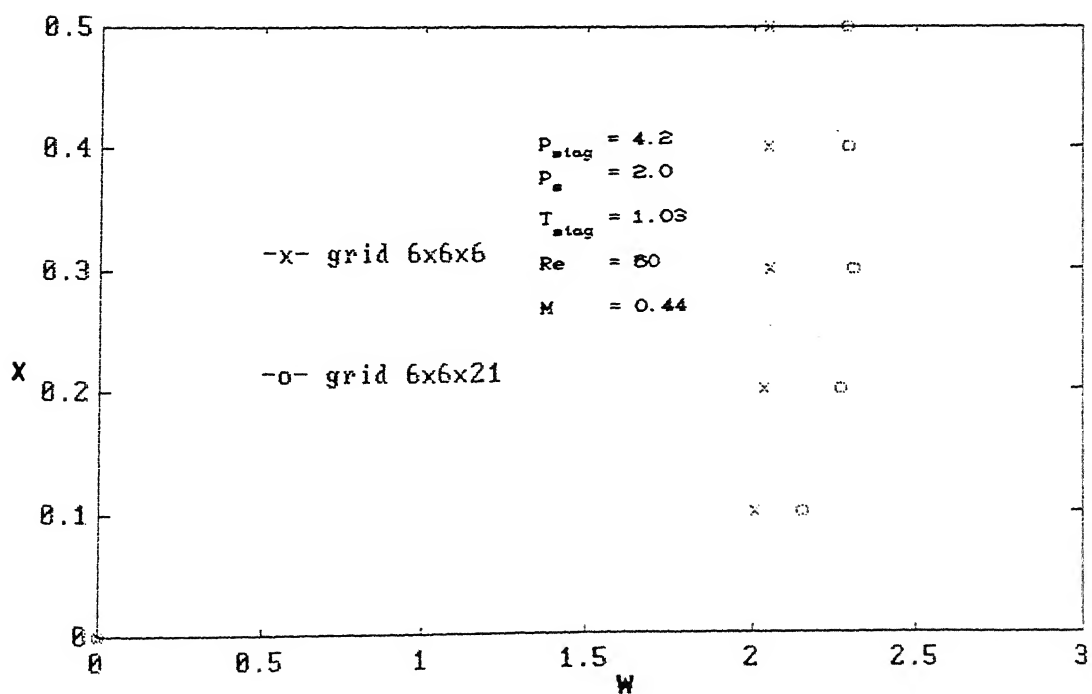


FIG 4.2 VARIATION OF COMPUTED AXIAL VELOCITY ALONG X
AT $Y = 0.5, Z = 0.5$

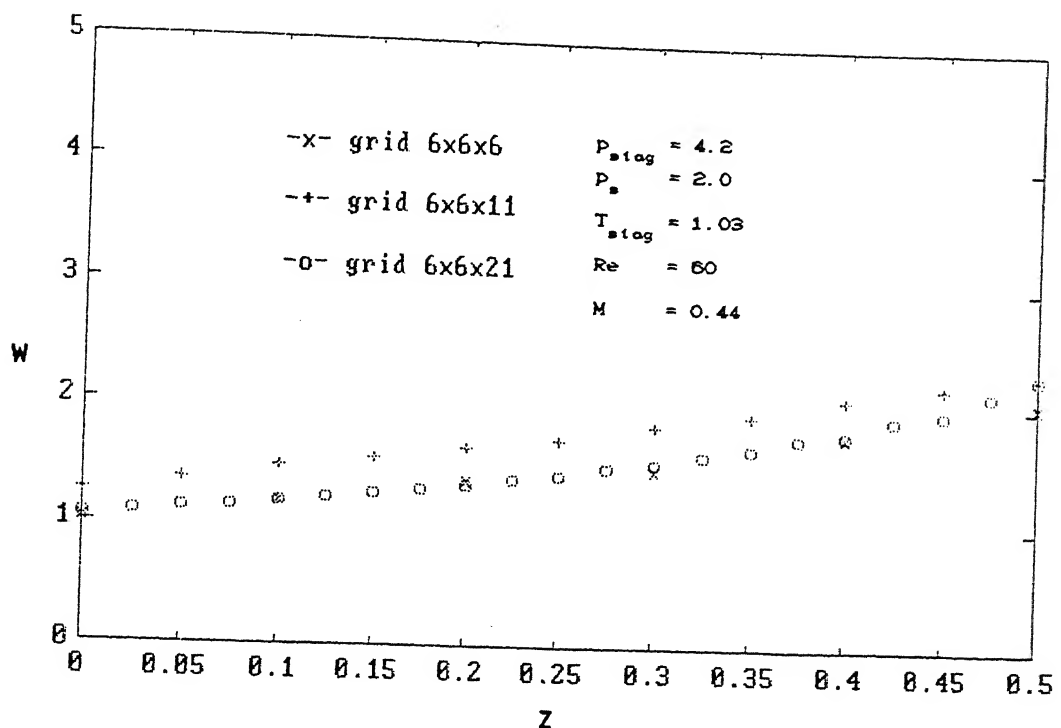


FIG 4.3 VARIATION OF COMPUTED CENTRELINE VELOCITY WITH AXIAL DISTANCE

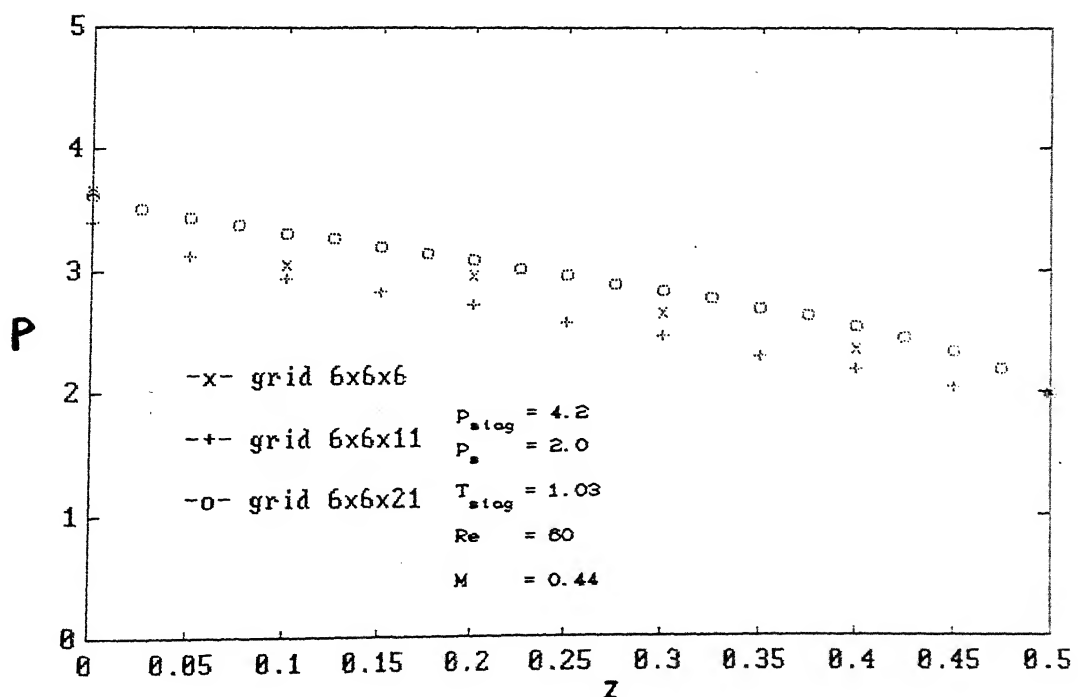


FIG 4.4 VARIATION OF COMPUTED CENTRELINE PRESSURE WITH AXIAL DISTANCE

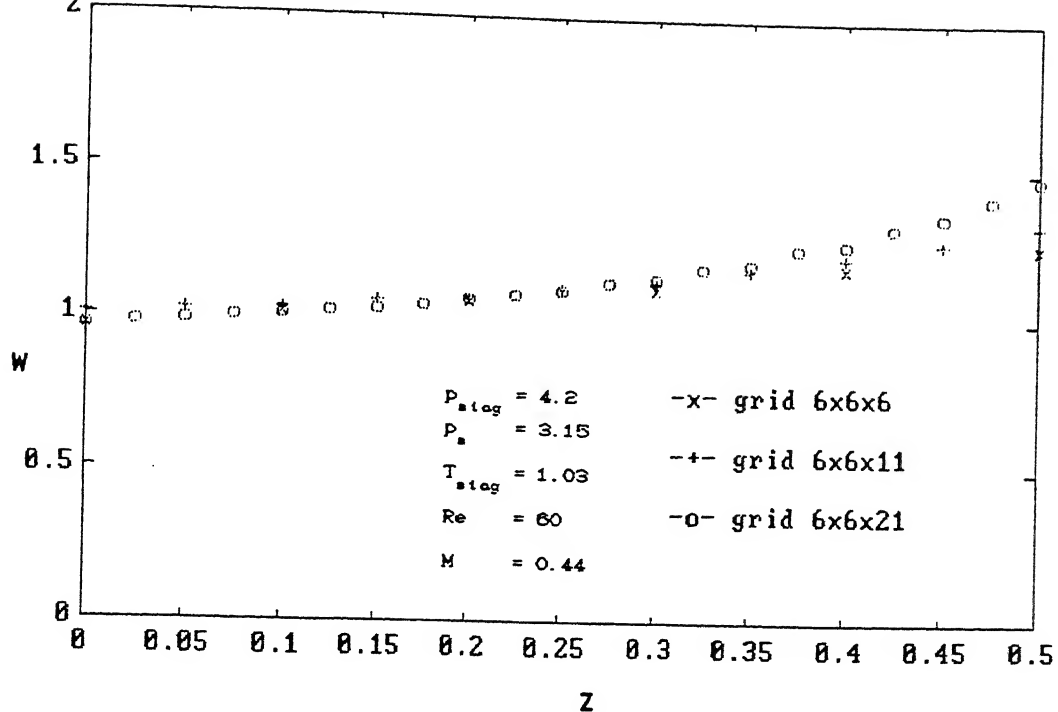


FIG 4.5 VARIATION OF COMPUTED CENTRELINE VELOCITY WITH AXIAL DISTANCE

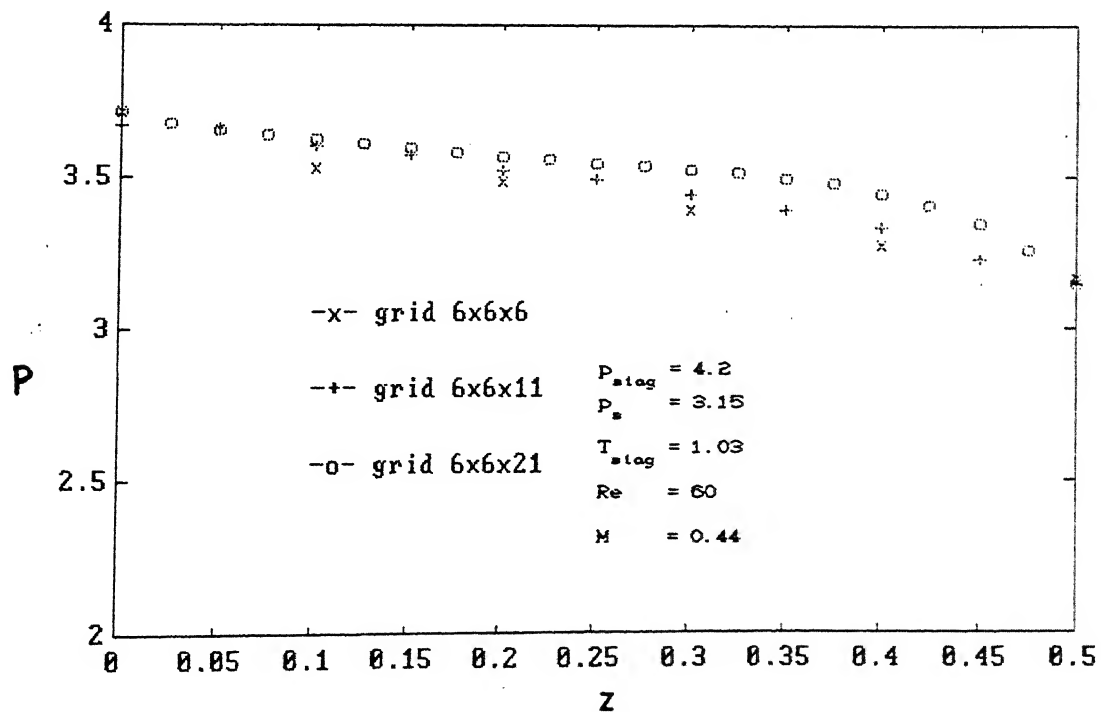


FIG 4.6 VARIATION OF COMPUTED CENTRELINE PRESSURE WITH AXIAL DISTANCE

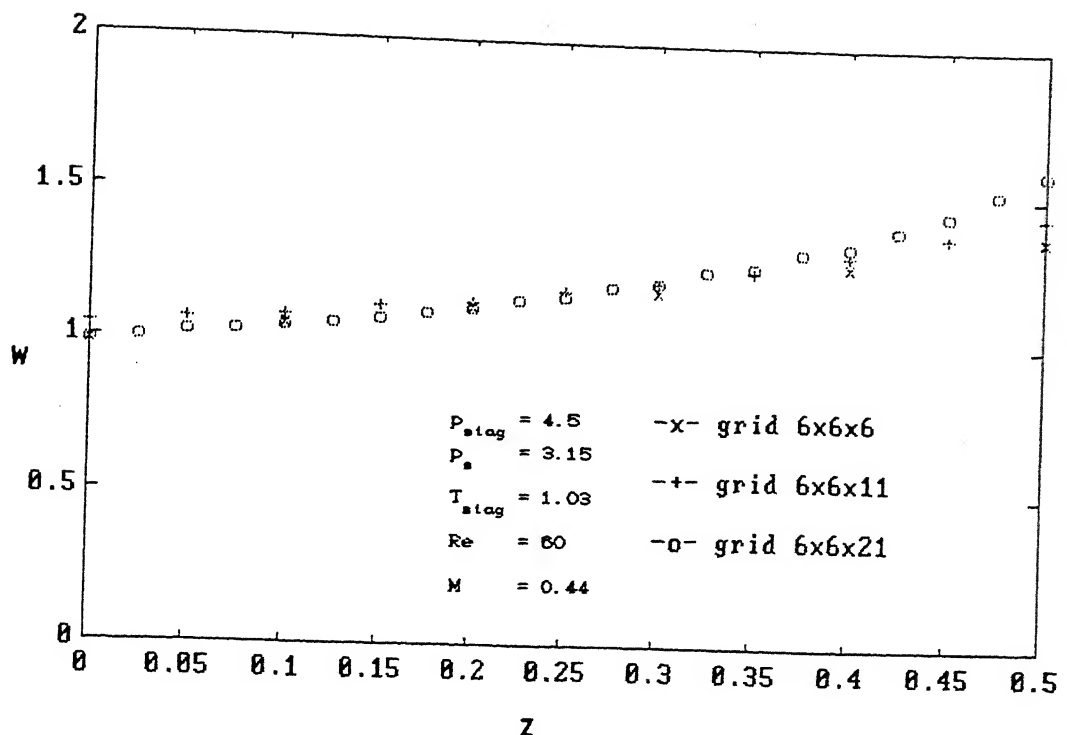


FIG 4.7 VARIATION OF COMPUTED CENTRELINE VELOCITY WITH AXIAL DISTANCE

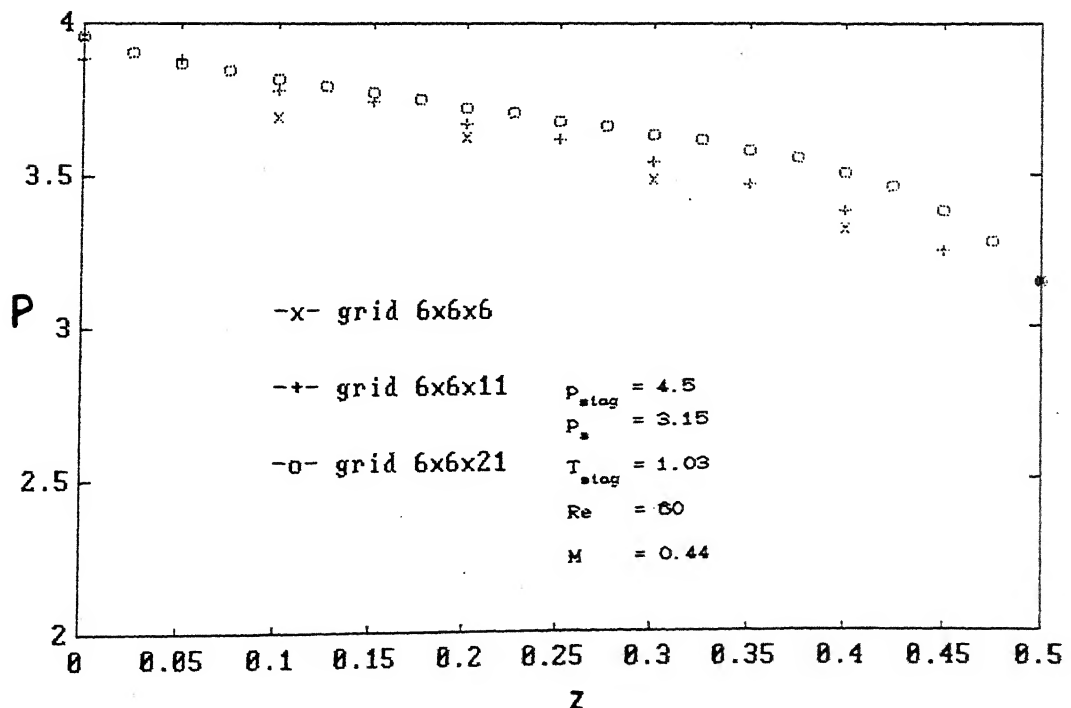


FIG 4.8 VARIATION OF COMPUTED CENTRELINE PRESSURE WITH AXIAL DISTANCE

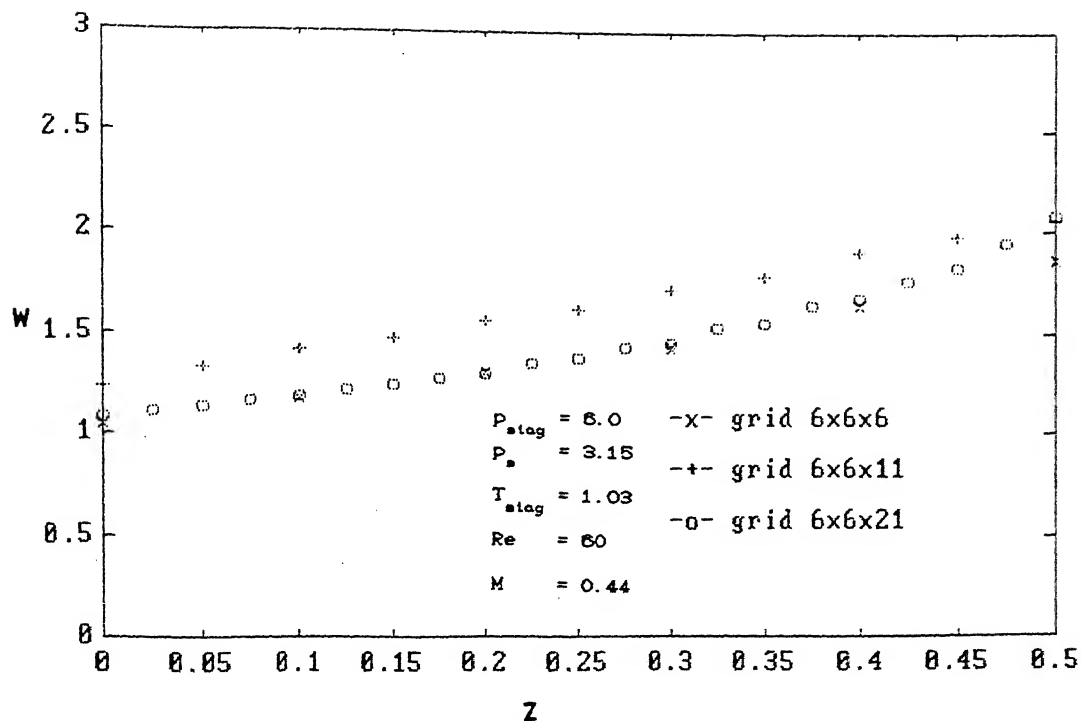


FIG 4.9 VARIATION OF COMPUTED CENTRELINE VELOCITY
WITH AXIAL DISTANCE

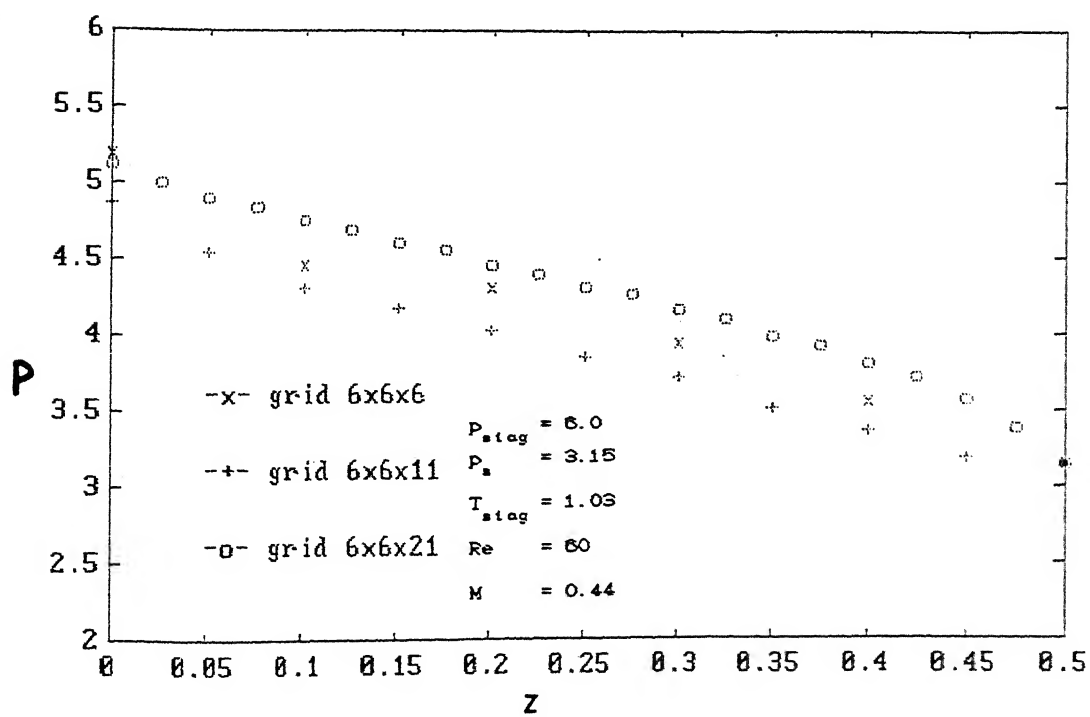


FIG 4.10 VARIATION OF COMPUTED CENTRELINE PRESSURE
WITH AXIAL DISTANCE

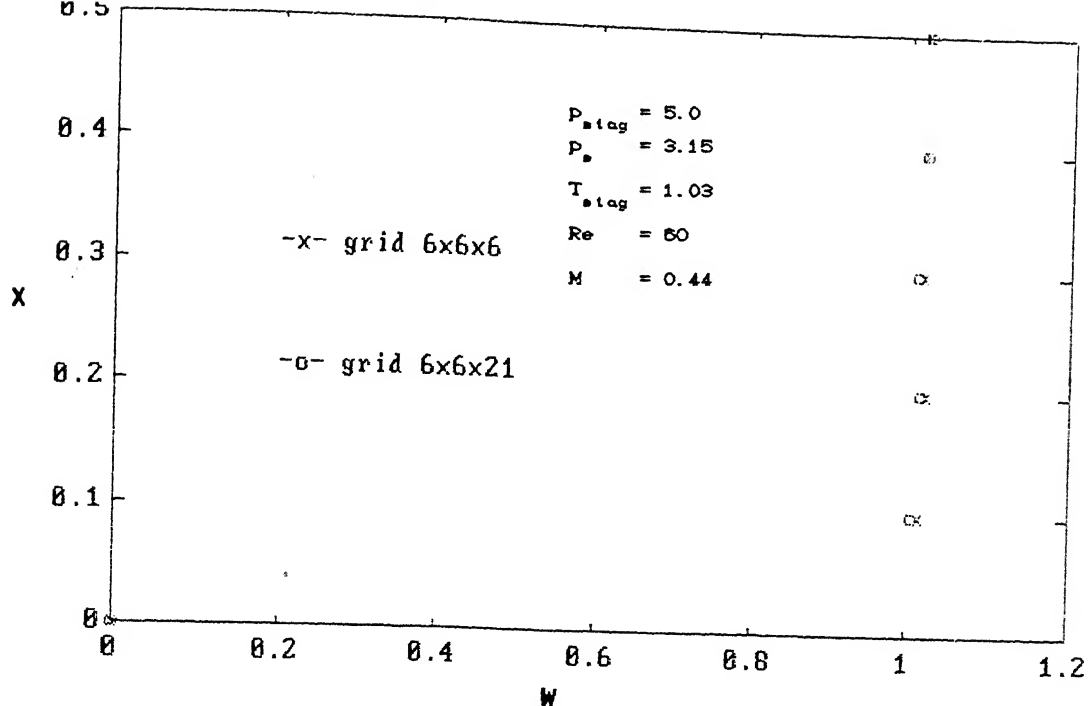


FIG 4.11 VARIATION OF COMPUTED AXIAL VELOCITY ALONG X
AT Y = 0.5, Z = 0

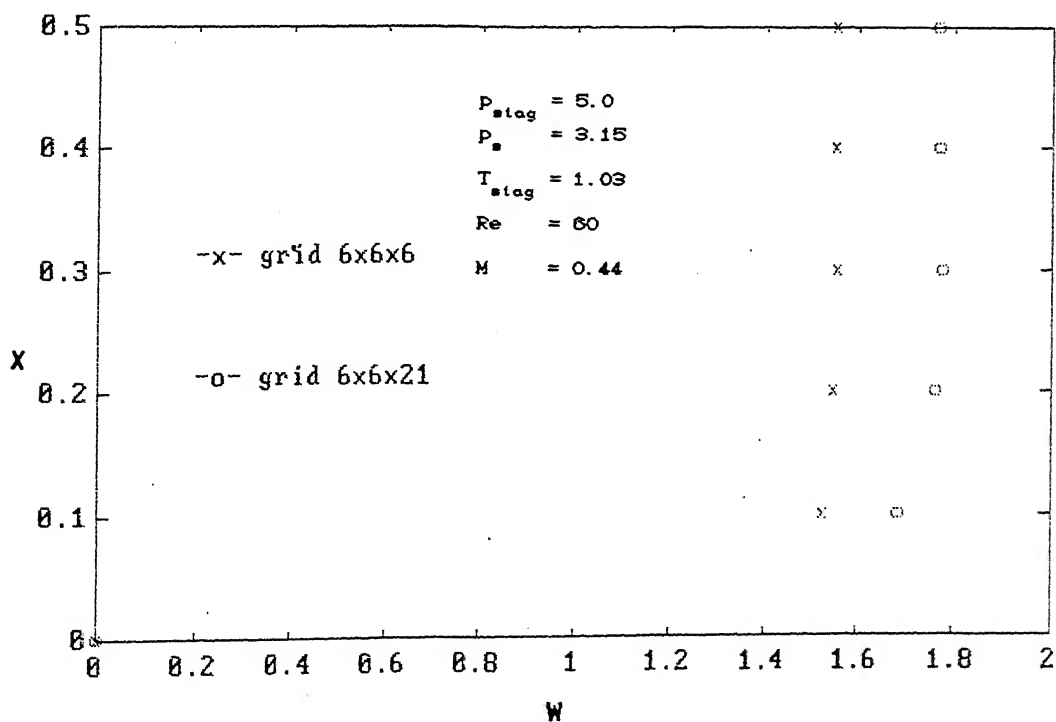


FIG 4.12 VARIATION OF COMPUTED AXIAL VELOCITY ALONG X

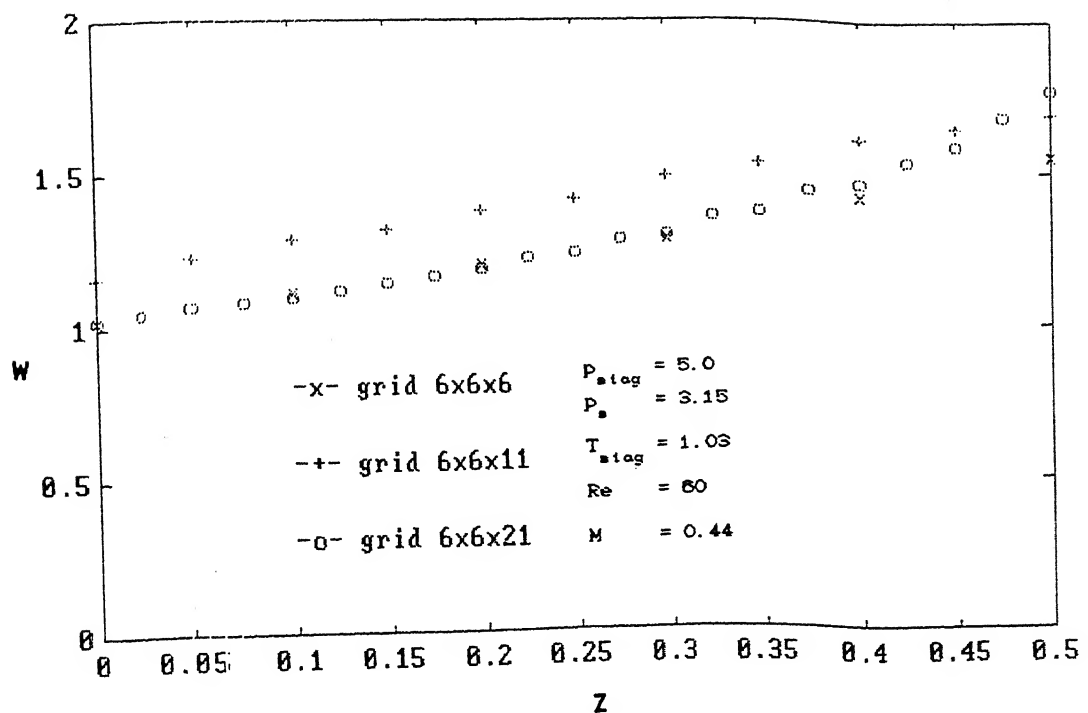
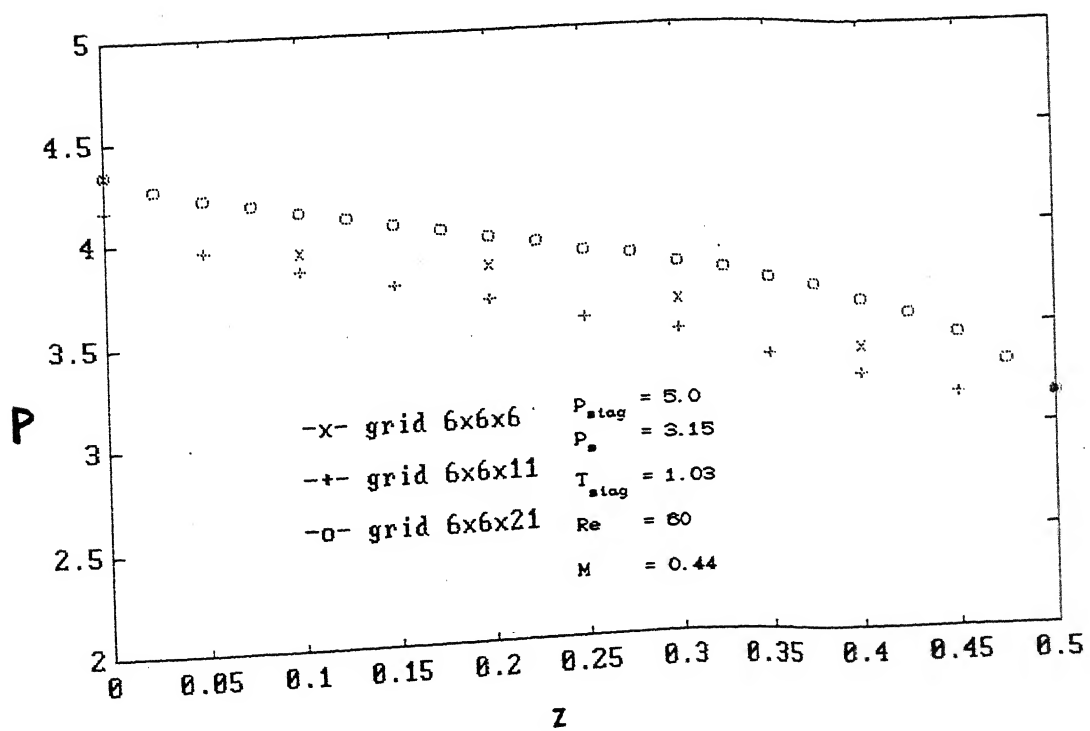


FIG 4.13 VARIATION OF COMPUTED CENTRELINE VELOCITY
WITH AXIAL DISTANCE



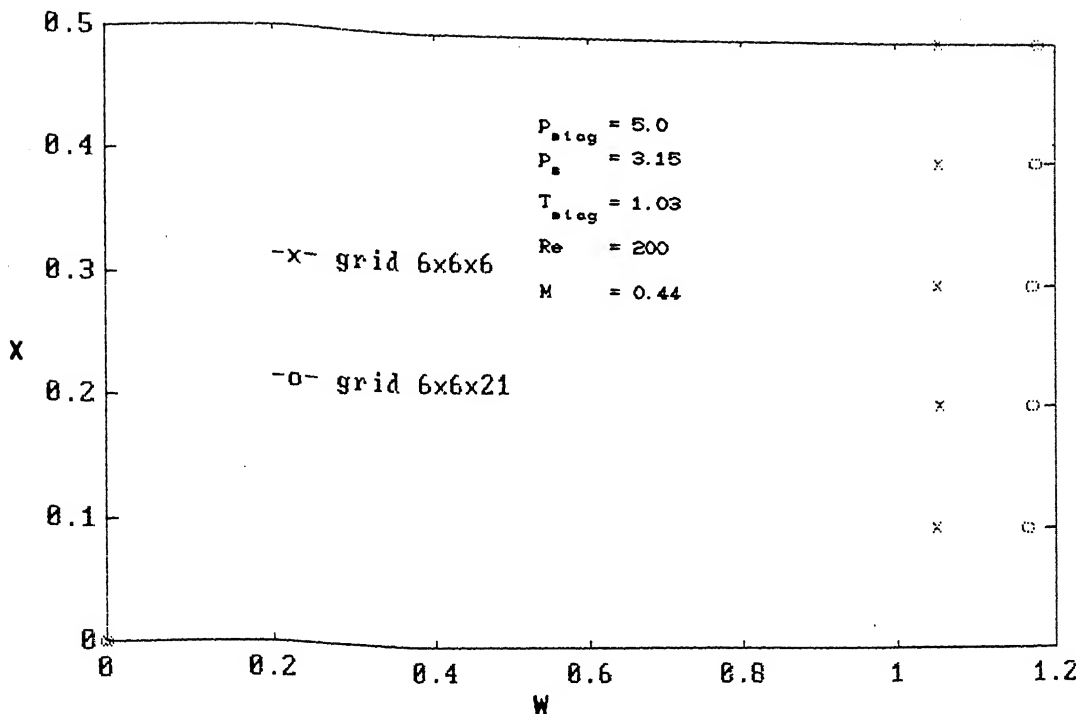


FIG 4.15 VARIATION OF COMPUTED AXIAL VELOCITY ALONG X
AT $Y = 0.5$, $Z = 0$

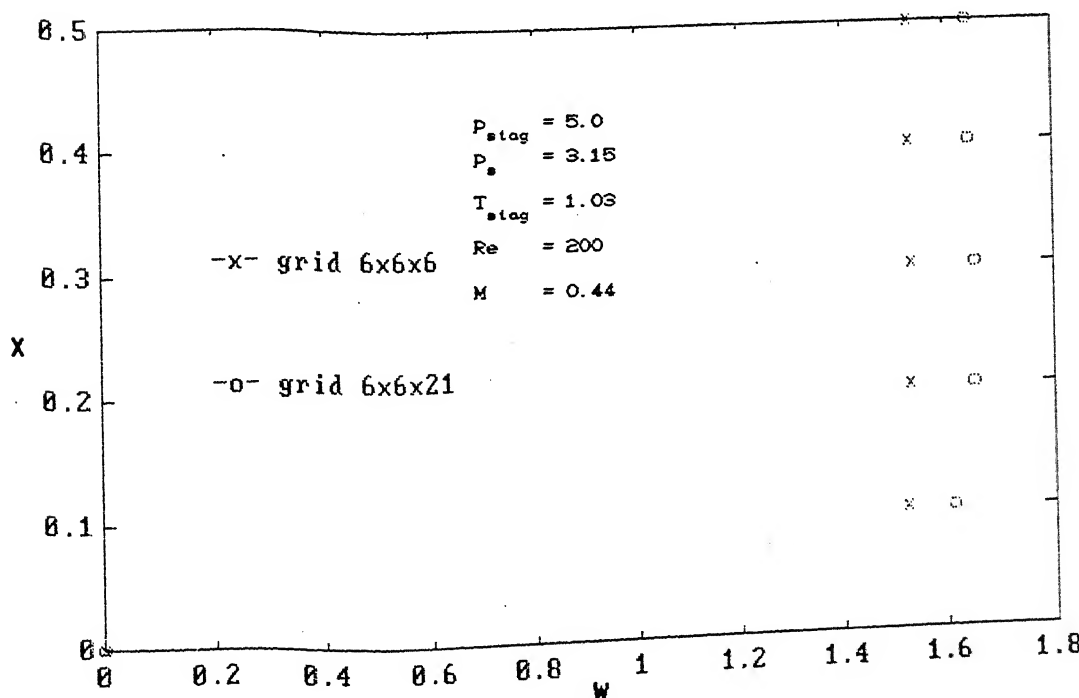


FIG 4.16 VARIATION OF COMPUTED AXIAL VELOCITY ALONG X
AT $Y = 0.5$, $Z = 0$

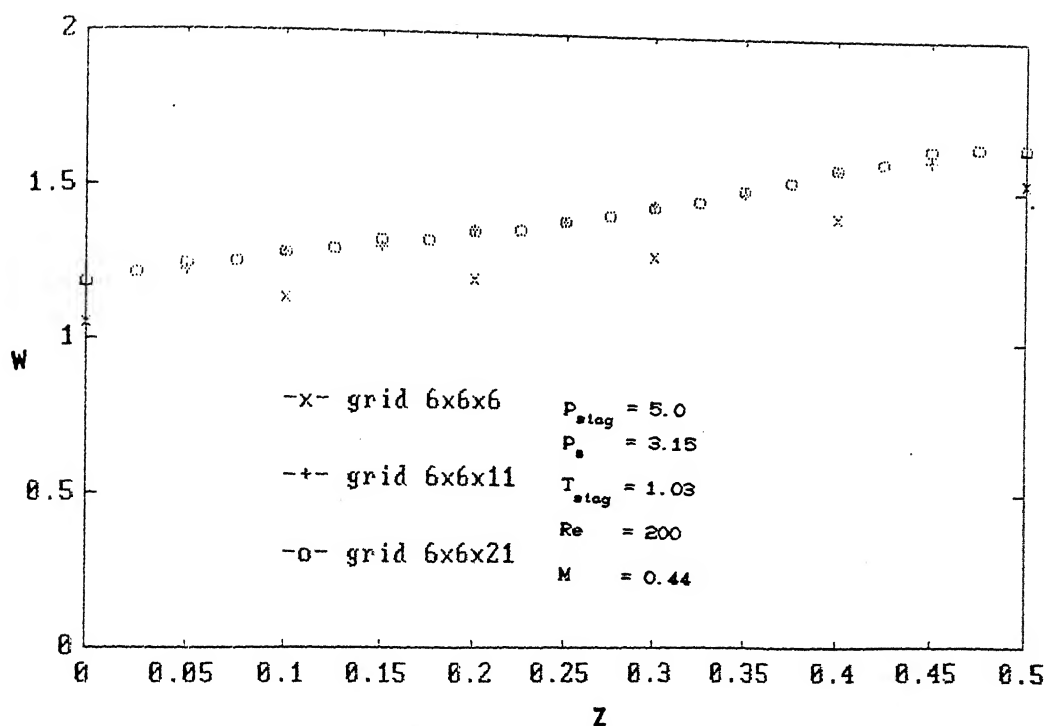


FIG 4.17 VARIATION OF COMPUTED CENTRELINE VELOCITY WITH AXIAL DISTANCE

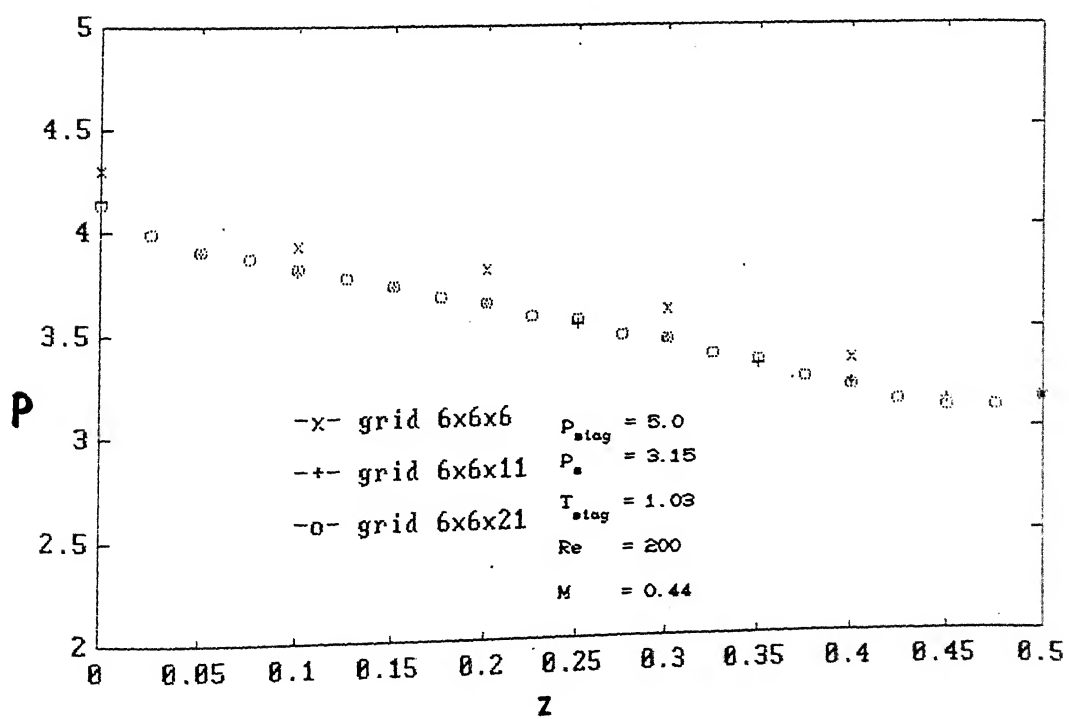


FIG 4.16 VARIATION OF COMPUTED CENTRELINE PRESSURE WITH AXIAL DISTANCE

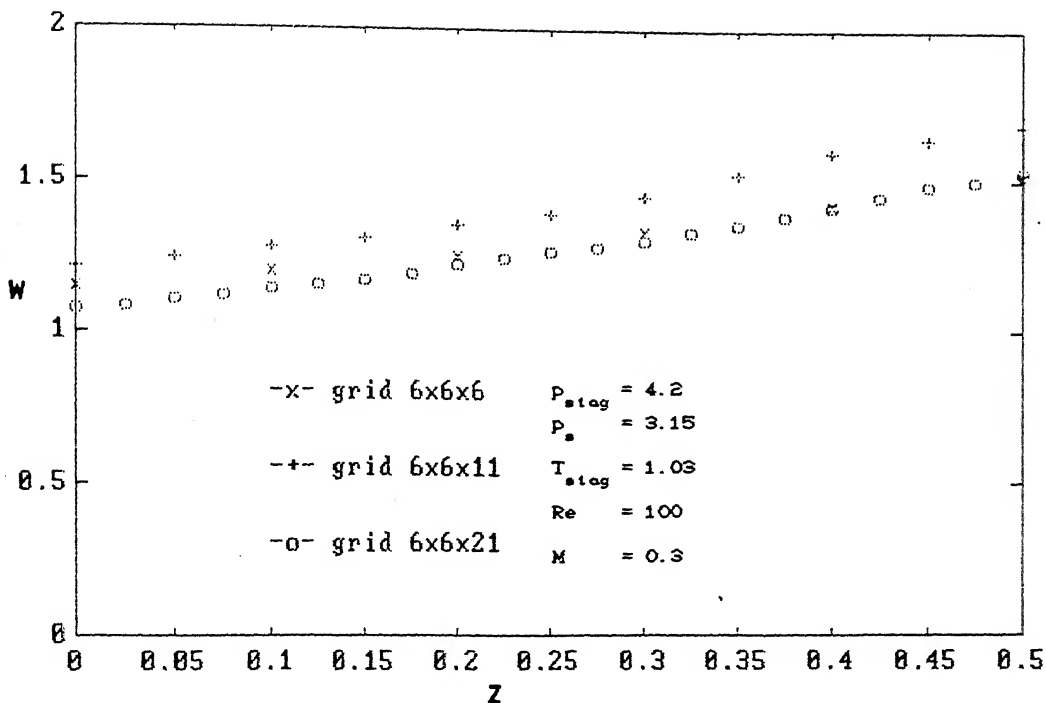


FIG 4.21 VARIATION OF COMPUTED CENTRELINE VELOCITY WITH AXIAL DISTANCE

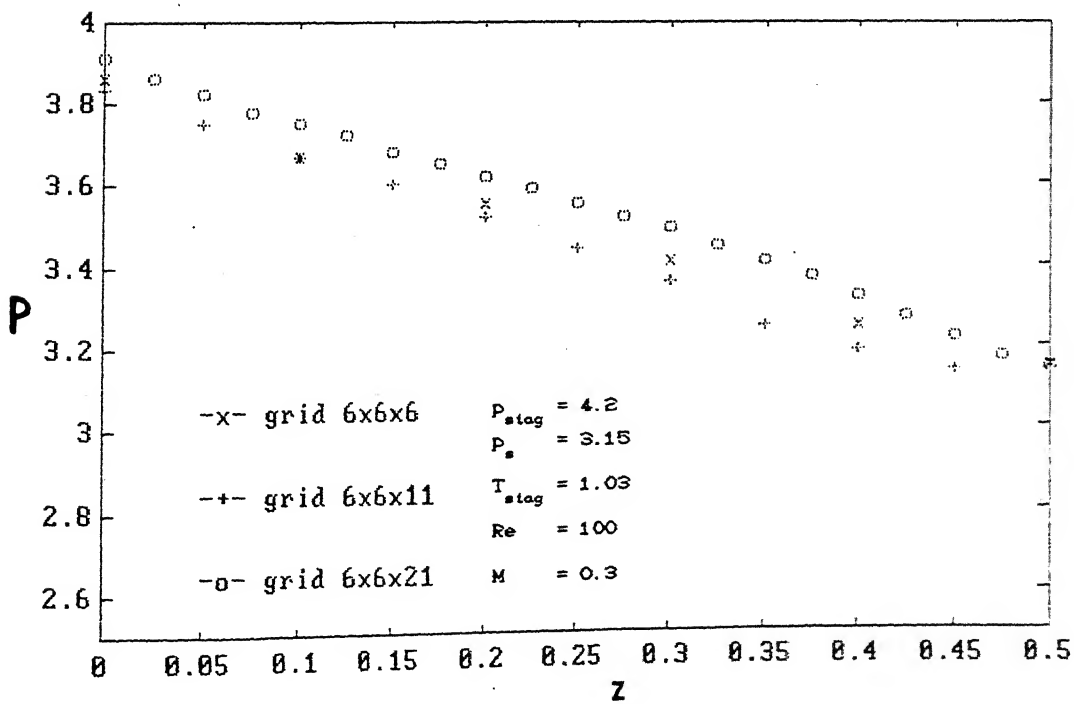


FIG 4.22 VARIATION OF COMPUTED CENTRELINE PRESSURE
WITH AXIAL DISTANCE

5. FUTURE WORK

been mentioned that, computer time with finer mesh sizes, is larger as compared to that with coarse mesh sizes. Also velocity gradients near the solid boundary are very large particularly for high Re. These suggest that it is desirable to use variable mesh size grid such that there are more number points near the solid boundaries. This may help in cutting down computer time.

, since in most real situations, the flow field is turbulent, an appropriate turbulent model may be incorporated in governing equations and the computer code modified accordingly.

Appendix I

Solution of Tridiagonal system of equations

$$\begin{matrix} d_0 & a_0 \\ b_1 & d_1 & a_1 \\ b_i & d_i & a_i \\ \vdots & & \end{matrix} \quad \text{O} \quad \left[\begin{array}{c} g_0 \\ g_1 \\ g_i \\ \vdots \\ g_L \end{array} \right] = \left[\begin{array}{c} r_0 \\ r_1 \\ r_i \\ \vdots \\ r_L \end{array} \right]$$

r the solution of above tridiagonal system equations " Thomas algorithm " is given as

r_i = 1 to L

$$= d_i - \frac{b_i}{d_{i-1}} a_{i-1}$$

$$= d_i - \frac{b_i}{d_{i-1}} a_{i-1}$$

$$= \frac{r_L}{d_L}$$

$i = L-1 \text{ to } 0$

$$= \frac{r_i - a_i g_{i+1}}{d_i}$$

Appendix II

Solution procedure for block-tridiagonal system of equations
[4.5]

$$\begin{bmatrix} A_0 & C_0 & & & \\ B_1 & A_1 & C_1 & & \\ & B_2 & A_2 & C_2 & \\ & & & \ddots & \\ & & & & B_L & A_L \end{bmatrix} \begin{bmatrix} G_0 \\ G_1 \\ G_2 \\ \vdots \\ G_L \end{bmatrix} = \begin{bmatrix} R_0 \\ R_1 \\ R_2 \\ \vdots \\ R_L \end{bmatrix} \quad (2.1)$$

where B, A, C are $(n \times n)$ matrices, R is a vector $(n \times 1)$, and G the column vector $(n \times 1)$ of variables. Solution procedure for the above system of equations is the following.

$$\begin{bmatrix} A_0 & C_0 & & & \\ B_1 & A_1 & C_1 & & \\ & B_2 & A_2 & C_2 & \\ & & & \ddots & \\ & & & & B_L & A_L \end{bmatrix} = \begin{bmatrix} I & \gamma_0 & & & & \\ & I & \gamma_1 & & & \\ & & I & \gamma_2 & & \\ & & & & \ddots & \\ & & & & & I \end{bmatrix} \quad (2.2)$$

where β 's, γ 's are $(n \times n)$ matrices and I's are the identity matrices. β 's and γ 's are determined as follows.

$$\beta_0 = A_0 \quad \beta_0 \gamma_0 = C_0$$

for $0 < i < L$

$$\beta_i = A_i - B_i \gamma_{i-1}, \quad \beta_i \gamma_i = C_i$$

$$\beta_L = A_L - B_L \gamma_{L-1}$$

$$\begin{bmatrix} I & \gamma_0 & & & \\ & I & \gamma_1 & & 0 \\ & & I & \gamma_2 & \\ & & & & \\ & 0 & & & I \end{bmatrix} \begin{Bmatrix} G_0 \\ G_1 \\ G_2 \\ \vdots \\ G_L \end{Bmatrix} = \begin{Bmatrix} \phi_0 \\ \phi_1 \\ \phi_2 \\ \vdots \\ \phi_L \end{Bmatrix} \quad (2.3)$$

Making use of (2.2) and (2.3), (2.1) may be expressed as

$$\begin{bmatrix} \beta_0 & & & & \\ B_1 & \beta_1 & & & 0 \\ B_2 & B_1 & \beta_2 & & \\ & & & & \\ 0 & & B_L & \beta_L & \end{bmatrix} \begin{Bmatrix} \phi_0 \\ \phi_1 \\ \phi_2 \\ \vdots \\ \phi_L \end{Bmatrix} = \begin{Bmatrix} R_0 \\ R_1 \\ R_2 \\ \vdots \\ R_L \end{Bmatrix} \quad (2.4)$$

ϕ 's are determined as follows

$$\beta_0 \phi_0 = R_0$$

$$\beta_1 \phi_1 = R_1 - B_1 \phi_{1-1}$$

$$\beta_L \phi_L = R_L - B_L \phi_{L-1}$$

for $0 < i < L$

Now from (2.3)

$$G_L = \phi_L$$

$$G_1 = \phi_1 - \gamma_1 G_{1+1} \quad \text{for } 0 < 1 < L$$

$$G_0 = \phi_0 - \gamma_0 G_1$$

CENTRAL LIBRARY
I.I.T., KANPUR
Rec No. A15420

APPENDIX III

Alternating direction Implicit Technique

$$A \zeta^{n+1} + \mathfrak{L}_x \zeta^{n+1} + \mathfrak{L}_y \zeta^{n+1} + \mathfrak{L}_z \zeta^{n+1} = \{ F \} \quad (3.1)$$

Here ζ is the column vector of dependent variables. \mathfrak{L}_x , \mathfrak{L}_y , \mathfrak{L}_z and A are the row vectors. \mathfrak{L}_x , \mathfrak{L}_y , \mathfrak{L}_z consist of partial differential operators with respect to x , y and z respectively.

ADI technique developed by Douglas-Gunn [1,6,7] when applied to the above partial differential equation gives

$$A \zeta^* + \mathfrak{L}_x \zeta^* = \{ F \} \quad (3.2)$$

$$A \zeta^{**} + \mathfrak{L}_y \zeta^{**} = A \zeta^* \quad (3.3)$$

$$A \zeta^{n+1} + \mathfrak{L}_z \zeta^{n+1} = A \zeta^{**} \quad (3.4)$$

For equation (3.2.5)

$$\zeta^{n+1} = \left\{ \psi_{\rho}^{n+1} \quad \psi_u^{n+1} \quad \psi_v^{n+1} \quad \psi_w^{n+1} \quad \psi_T^{n+1} \right\}^T$$

$$A = \{ 1 \quad 0 \quad 0 \quad 0 \quad 0 \}$$

$$\mathfrak{L}_x = \left\{ \Delta t \frac{\partial u^n}{\partial x} + \Delta t u^n \frac{\partial}{\partial x} \quad \Delta t \frac{\partial \rho^n}{\partial x} + \Delta t \rho^n \frac{\partial}{\partial x} \quad 0 \quad 0 \quad 0 \right\}$$

$$\mathfrak{L}_y = \left\{ \Delta t \frac{\partial v^n}{\partial y} + \Delta t v^n \frac{\partial}{\partial y} \quad 0 \quad \Delta t \frac{\partial \rho^n}{\partial y} + \Delta t \rho^n \frac{\partial}{\partial y} \quad 0 \quad 0 \right\}$$

$$\mathfrak{L}_z = \left\{ \Delta t \frac{\partial w^n}{\partial z} + \Delta t w^n \frac{\partial}{\partial z} \quad 0 \quad 0 \quad \Delta t \frac{\partial \rho^n}{\partial z} + \Delta t \rho^n \frac{\partial}{\partial z} \quad 0 \right\}$$

$$F = - \Delta t \left(\frac{\partial (\rho u)^n}{\partial x} + \frac{\partial (\rho v)^n}{\partial y} + \frac{\partial (\rho w)^n}{\partial z} \right)$$

 REFERENCES

- 1. W. R. BRILEY AND H. McDONALD, Solution of Multidimensional compressible Navier-Stokes Equations by a Generalized Implicit method, Journal of Computational Physics 24, p. 372-397 (1977)
- 2. Computational Fluid Mechanics and Heat transfer, DALE A. ANDERSON, JOHN C. TANNEHILL, RICHARD H. PLETCHER, Hemisphere publishing Corporation.(1984)
- 3. Elements of Gas Dynamics, H. W. LIEPMANN AND A. ROSHKO, Wiley, New York.(1957)
- 4. Analysis of Turbulent Boundary Layers, TUNCER CEBECI AND A. M. SMITH, Academic Press.(1974)
- 5. Analysis of Numerical Methods, E. ISAACSON AND H. B. KELLER, Wiley.(1966)
- 6. Numerical Methods For Partial Differential equations, WILLIAM AMES, Academic Press.(1977)
- 7. DOUGLAS J. Jr. , AND J. E. GUNN, A General formulation of Alternating Direction Methods, Part 1, Parabolic and Hyperbolic problems, Numerische Mathematik,p.428, Band 6 (1964)
- 8. Finite Element Programming of the Navier-Stokes Equation, C. TAYLOR, T. G. HUGHES, Pineridge Press Limited, Swansea, U. K. 1981)
- 9. Manuscript " Computational Heat Transfer ", YOGESH JALURIA, Department of Mechanical Engineering, I.I.T., Kanpur.(1980)